Learning Optimized Risk Scores from Large-Scale Datasets

Berk Ustun ustunb@mit.edu
Department of Electrical Engineering and Computer Science
Massachusetts Institute of Technology

Cynthia Rudin cynthia@cs.duke.edu
Department of Computer Science
Duke University

arXiv:1610.00168v2 [stat.ML] 1 Nov 2016

Abstract

Risk scores are simple classification models that let users quickly assess risk by adding, subtracting and multiplying a few small numbers. These models are used for high-stakes applications in healthcare and criminology, but difficult to build because they need to be risk-calibrated, use a few small integer coefficients, and obey operational constraints. In this paper, we present a new approach to learn risk scores that are fully optimized for feature selection, integer coefficients, and operational constraints. We formulate the risk score problem as a mixed integer nonlinear program, and present a new cutting plane algorithm to efficiently recover its optimal solution while avoiding the stalling behavior of existing cutting plane algorithms on non-convex problems. We pair our cutting plane algorithm with specialized techniques to generate feasible solutions, narrow the optimality gap, and reduce data-related computation. The resulting approach can learn optimized risk scores in a way that scales linearly in the number of samples, provides a proof of optimality, and accommodates complex operational constraints. We illustrate the benefits of our approach through extensive numerical experiments.

Keywords: classification; cutting plane methods; discrete optimization; mixed integer non-linear programming; risk assessment; scoring systems;

1. Introduction

Risk scores are simple linear classification models that let users assess risk by adding, subtracting, and multiplying a few small numbers. These models are widely used for high-stakes applications in medicine and criminology because they let users make quick predictions, without extensive training, and without the use of a computer or calculator. The nature of such applications means that risk scores have to be rank-accurate (i.e., high AUC), risk-calibrated, sparse, and use small integer coefficients. In addition, domain experts may require risk scores to satisfy operational constraints to be deployed, such as limits on model size ("the model should use at most 4 features"), feature composition ("if the model uses *hypertension*, then it should also use $bmi \geq 25$"), and prediction ("the model should *not* predict that males have higher risk than females").

In spite of their extensive use in high-stakes applications, there is currently no principled approach to learn risk scores from data. Existing models are created ad hoc, either by a panel of experts (see e.g., the CHADS_2 score of Gage et al., 2001) or by combining heuristics (e.g. rounding logistic regression coefficients after manual feature selection, as recommended by the U.S. Department of Justice, 2005). These approaches may produce risk scores with poor rank-accuracy or risk calibration compared to the state-of-the-art (see

e.g., the performance of $CHADS_2$ in Letham et al. 2013). As we show, modern methods for penalized logistic regression (Efron et al., 2004; Zou and Hastie, 2005) are also ill-suited to create risk scores as they must be paired with a rounding heuristic to produce models with small integer coefficients. The resulting approach combines multiple approximations, depends on extensive parameter tuning, and provides no guarantee as to whether it can produce a feasible risk score, let alone one that is optimal. In practice, the lack of a formal guarantee makes it difficult to navigate trade-offs between model form and model performance, as practitioners cannot tell if poor performance is due to restrictive constraints on model form, or lax approximations used in the approach to determine the coefficients.

Our goal in this paper is to present a principled approach to learn risk scores by solving a discrete optimization problem, namely the *risk score problem*. We consider a mixed integer nonlinear program (MINLP) that minimizes the logistic loss (for rank accuracy and risk calibration), penalizes the ℓ_0-norm (for sparsity), and uses discrete variables to restrict coefficients to small integers and enforce operational constraints. We refer to the risk score built by solving this problem as a *Risk-calibrated Supersparse Linear Integer Model* (RiskSLIM). Unlike existing approaches, our approach is designed to fit models that are fully optimized for feature selection, small integer coefficients, and operational constraints. In addition, it provides a simple mechanism to address operational constraints without parameter tuning or post processing, by explicitly including these constraints in the MINLP formulation. In light of these benefits, a key part of our approach hinges on solving the risk score problem to optimality (i.e., to recover the optimal solution and pair it with a certificate of optimality). By design, the optimal solution to the risk score problem attain the best performance among a class of models that satisfy a fixed set of constraints. Therefore, by solving this problem to optimality, we either obtain a risk score with suitable performance, or a certificate to show that the constraints were overly restrictive.

As we show, solving the risk score problem to optimality with an off-the-shelf MINLP solver is time-consuming even for small datasets, as generic algorithms designed to handle a wide class of MINLPs are slowed down by excessive data-related computations for our problem. Accordingly, we solve the risk score problem with a *cutting plane algorithm*, which can reduces data-related computation by iteratively solving a surrogate of the problem contains a piecewise-linear approximation of the loss function. Cutting-plane algorithms have an impressive track record in solving large-scale supervised learning problems (see Teo et al., 2007, 2009; Franc and Sonnenburg, 2008; Joachims et al., 2009), as they scale linearly with the number of samples in the dataset and provide fine-grained control over data-related computation. Unfortunately, existing cutting plane algorithms are designed under the assumption that the surrogate optimization problem can be solved to optimality at each iteration. Although this is perfectly reasonable in a convex setting, it leads cutting plane algorithms to *stall* on non-convex problems, meaning that they spend too much time solving the surrogate problem to optimality before converging. We demonstrate the stalling phenomenon, and present a cutting plane algorithm to overcome this issue, called the *lattice cutting plane algorithm*. The resulting approach extends the benefits of cutting plane algorithms to discrete optimization problems, allowing us to learn optimized risk scores in a way that scales linearly in the number of samples, provides a certificate of optimality, and complex operational constraints needed for these models to be deployed.

Contributions

The main contributions of this paper are as follows.

- We propose a new approach to build risk scores that are fully optimized for feature selection, small integer coefficients, and operational constraints. Our approach has the benefit that it can produce simple models without parameter tuning or post processing, and pair all models with a certificate of optimality.
- We present a new cutting plane algorithm for discrete optimization problems, called the lattice cutting plane algorithm. Our algorithm retains the scalability and flexibility of cutting plane algorithms designed for convex optimization problems, but does not stall as they do on non-convex optimization problems.
- We improve the performance of LCPA for the risk score problem by designing specialized techniques to: (i) generate and polish integer feasible solutions; (ii) improve the rate of convergence; (iii) reduce data-related computation. The procedures in (i) can be used to produce risk scores with superior performance in a heuristic approach.
- We benchmark risk scores built using several principled approaches on publicly available datasets. Our results show that we can use our approach to fit optimized risk scores in minutes. In addition, they highlight pitfalls of heuristics that are used in practice and show implicit trade-offs between performance and form.
- We provide software to create optimized risk scores using Python and the CPLEX API.

Structure

Our paper is structured as follows. In Section 1.1, we discuss related work. In Section 2, we formally describe the risk score problem. In Section 3, we briefly review existing cutting plane algorithms, and present our proposed cutting plane algorithm to solve non-convex optimization problems without stalling (LCPA). In Sections 4 and 5, we present specialized techniques to improve the performance of LCPA for the risk score problem. In Section 6, we present experimental results to benchmark risk scores built using various data-driven methods in terms of rank-accuracy and risk calibration. In the appendices, we include: proofs of all theorems (Appendix A); details on our implementation (Appendix B); details on the experiments from Sections 3 – 5 (Appendix C) .

1.1 Related Work

In what follows, we discuss related work in risk scores, machine learning, and optimization.

Risk Scores

Starting with the work of Burgess (1928), simple risk scores have been used in many high-stakes applications. Examples in criminology include: the Ohio Risk Assessment System (Latessa et al., 2009); the Kentucky Pretrial Risk Assessment Instrument (Austin et al., 2010); and the Offense Gravity Score (Pennsylvania Commission on Sentencing, 2012). Examples in medicine include: SAPS I, II, III (Le Gall et al., 1984, 1993; Moreno et al., 2005) and APACHE I, II, III (Knaus et al., 1981, 1985, 1991) to assess ICU mortality risk.

Risk scores with few terms and small integer coefficients are often preferred for these applications due to their high level of interpretability and their ability to make predictions without a computer or a calculator. Duwe and Kim (2016), for example, write: "*It is commonplace... for fine-tuned regression coefficients to be replaced with a simple-point system... to promote the easy implementation, transparency, and interpretability of risk-assessment instruments.*" Ridgeway (2013) provides similar reasons to justify why the LAPD uses a simple risk score to identify recruits who may become officers: "*A decent transparent model that is actually used will outperform a sophisticated system that predicts better but sits on a shelf. If the researchers had created a model that predicted well but was more complicated, the LAPD likely would have ignored it, thus defeating the whole purpose.*" Interpretability has become a crucial requirement for models used in high-stakes applications (Kodratoff, 1994), as evidenced by upcoming European Union regulations that mandate a "right to an explanation" from algorithmic decision-making tools (Goodman and Flaxman, 2016).

The lack of a principled methodology to create risk scores is best evidenced by the number of ad hoc approaches that are used in practice (see e.g., the review of Bobko et al., 2007). Existing tools are built by combining heuristics for fitting, rounding and feature selection. Examples include: (i) having a panel of experts build a model by hand and only using data to validate the model as it is built (see e.g., Gage et al., 2001); (ii) creating a risk score by adding together input variables that are strongly correlated with the outcome variable (i.e., the *Burgess* method as it was first used by Burgess, 1928); (iii) rounding the coefficients of a logistic regression model (Goel et al., 2015) or a linear probability model (U.S. Department of Justice, 2005) – sometimes referred to as the *weighted Burgess* method. Risk scores built using ad hoc approaches can perform poorly compared to models built using modern data-driven methods (see e.g., the poor performance of CHADS_2 in Letham et al. 2013, as well as risk scores built with the Burgess method in Duwe and Kim 2016).

Given the prevalence of ad hoc approaches to create risk scores, a minor contribution of this work are heuristic data-driven methods to build and evaluate risk scores (i.e., the baseline methods in Section 6 that learn risk scores from data by pairing ℓ_1/ℓ_2 penalized logistic regression with various rounding and polishing techniques).

Machine Learning

The RiskSLIM models in this paper have the same form as the SLIM models in Ustun and Rudin (2015), but differ in the way they are used and built. RiskSLIM models are designed for risk assessment and built by solving a mixed-integer nonlinear program (MINLP) that optimizes the logistic loss. In contrast, SLIM models are designed for decision-making and built by solving a mixed-integer linear program (MIP) that optimizes the 0–1 loss. Optimizing the 0–1 loss does not necessarily produce models that are risk-calibrated or rank accurate. Optimizing the 0–1 loss is also $\mathcal{NP}$-hard (Nguyen and Sanner, 2013), meaning that SLIM does not scale to problems with large sample sizes as is the case here.

Our risk score problem resembles the one in Ertekin and Rudin (2015) in that it minimizes the logistic loss, penalizes the ℓ_0-norm, and restricts coefficients to a discrete set. Ertekin and Rudin (2015) solve this problem approximately using a Bayesian approach, which has a benefit in that it produces a posterior distribution on the coefficients. In contrast, we use an optimization approach, which can consistently recover a globally optimal

solution, and fit models that obey operational constraints. We pair our approach with new techniques to generate feasible solutions and reduce data-related computation, which results in a substantially more efficient approach than that of Ertekin and Rudin (2015).

Our cutting plane algorithm could be extended to generally solve risk minimization problems that minimize a convex loss function with non-convex regularizers and/or over non-convex feasible regions. Potential problems include ℓ_0-regularized risk minimization, or discrete linear classification problems that minimize the hinge loss over a small set of integers (Chevaleyre et al., 2013; Malioutov and Varshney, 2013; Carrizosa et al., 2016).

Optimization

We fit risk scores by solving a MINLP with three main components: (i) a convex loss function; (ii) a non-convex regularization penalty; (iii) a discrete and bounded feasible region. In Section 3.3, we argue that this MINLP needs to be solved with a specialized algorithm as off-the-shelf MINLP solvers fail to solve instances for small datasets. Recent work in optimization has focused on methods to solve problems that contain some – but not all – of these components. The quadratic integer programming method of Park and Boyd (2015a), for instance, can be extended to handle problems with a convex loss but cannot handle a non-convex regularizer. Similarly, Hübner and Schöbel (2014) provide sufficient conditions to recover an integer minimizer to a nonlinear optimization problem by rounding its fractional minimizer. However, these conditions do not hold for our problem due to additional non-convexities imposed by the ℓ_0-penalty and operational constraints.

We solve the risk score problem with a cutting plane algorithm, which have been extensively studied by the optimization community (see e.g., Kelley, 1960), and successfully used to solve large-scale supervised learning problems (Teo et al., 2007, 2009; Franc and Sonnenburg, 2008, 2009). Our algorithm makes use of callbacks in modern MIP solvers, which can dynamically add cutting planes in a branch-and-bound tree (see e.g., Bai and Rubin, 2009; Naoum-Sawaya and Elhedhli, 2010, for similar uses of callbacks in the optimization literature). LCPA differs from existing algorithms in that it does not *stall* on non-convex problems (i.e., it does not spend too much time solving a surrogate optimization problem to optimality before converging). As we explain in Section 3.1, many cutting plane algorithms will stall on non-convex problems including those that are not used for machine learning applications (see Boyd and Vandenberghe, 2004, for a list).

2. Problem Statement

Our goal is to build risk assessment tools (i.e., *risk scores*) such as the one in Figure 1.

1.	*Congestive Heart Failure*	1 point		.....
2.	*Hypertension*	1 point	+	.....
3.	*Age* $\geq$ *75*	1 point	+	.....
4.	*Diabetes Mellitus*	1 point	+	.....
5.	*Prior Stroke or Transient Ischemic Attack*	2 points	+	.....
	ADD POINTS FROM ROWS 1 – 5	**SCORE**	=	.....

SCORE	0	1	2	3	4	5	6
RISK	1.9%	2.8%	4.0%	5.9%	8.5%	12.5%	18.2

Figure 1: CHADS_2 risk score of Gage et al. (2001) for assessing stroke risk.

We formalize this problem as follows. We start with a dataset of N i.i.d. training examples $\{(\boldsymbol{x}_i, y_i)\}_{i=1}^N$ where $\boldsymbol{x}_i \subseteq \mathbb{R}^{d+1}$ denotes a vector of features $[1, x_{i,1}, \ldots, x_{i,d}]^T$ and $y_i \in \{\pm 1\}$ denotes a class label. We consider a linear score function $s(\boldsymbol{\lambda}, \boldsymbol{x}) = \langle \boldsymbol{\lambda}, \boldsymbol{x} \rangle$ where $\boldsymbol{\lambda} \subseteq \mathbb{R}^{d+1}$ is a vector of coefficients $[\lambda_0, \lambda_1, \ldots, \lambda_d]^\top$, and λ_0 is an intercept term. We estimate the *predicted risk* that example i belongs to the positive class using the logistic link function as

$$\Pr\left(y_i = +1 \mid \boldsymbol{x}_i\right) = \frac{1}{1 + \exp(-\langle \boldsymbol{\lambda}, \boldsymbol{x}_i \rangle)}.$$

In this setup, each coefficient λ_j represents the number of points for a given feature. Given an example with features $\boldsymbol{x}_i$, users tally the points to obtain a total score $s_i := \langle \boldsymbol{\lambda}, \boldsymbol{x}_i \rangle$, and use the total score s_i to obtain an estimate of predicted risk. Alternatively, users can obtain a predicted label $\hat{y}_i \in \{\pm 1\}$ by comparing the predicted risk to a threshold risk (e.g., predict $\hat{y}_i = +1$ if and only if $\Pr\left(y_i = +1\right) > 50\%$).

In practice, the desirable characteristics of a risk score include all of the following:

- *Rank Accuracy*: A rank-accurate model is a model with high AUC. Such a model outputs scores that can be used to order examples in terms of their true risk.
- *Risk Calibration*: A risk-calibrated model yields risk predictions that match observed risk. A risk-calibrated model will have high AUC, but the converse is not true.
- *Sparsity and Small Integer Coefficients*: linear models that use a few small integer coefficients allow for quick predictions without a computer or calculator. These models also help users gauge the influence of each input variable, and understand how multiple input variables are used to produce an estimate of predicted risk – especially because humans have severe difficulties when handling multiple cognitive entities (at most 4 according to Cowan 2010, which updates the estimate of 7 ± 2 from Miller 1984) as well as estimating associations between multiple variables (3 or more according to Jennings et al., 1982).

Building risk scores involves trade-offs between model performance (i.e., AUC and risk calibration) and model form (i.e., sparsity and small integer coefficients). We expect to sacrifice some performance by constraining models to use a few small integer coefficients. We expect to recover this as we relax various constraints on model form (see e.g., the trade-offs between model size, AUC and risk calibration in Figures 14 and 15 from Section 6).

In practice, finding a model that strikes an acceptable balance between performance and form is particularly difficult for this problem because: (i) AUC and risk calibration are potentially competing objectives (see Caruana and Niculescu-Mizil, 2006, for a discussion); (ii) restricting coefficients to a small integers may not impact performance for small models (i.e., $\|\boldsymbol{\lambda}\|_0 \leq 5$); (iii) some constraints on model form may be desirable because they mitigate overfitting; (iv) the trade-off is difficult to predict when models have to obey additional operational constraints. Current approaches address sparsity and integer coefficients through approximations, and therefore cannot guarantee a pareto-optimal model.

Risk Score Problem

We learn the values of the coefficients from data by solving the following mixed integer nonlinear program (MINLP), which we refer to as the *risk score problem* or RiskSlimMINLP:

$$\begin{aligned} \min_{\boldsymbol{\lambda}} \quad & l(\boldsymbol{\lambda}) + C_0 \|\boldsymbol{\lambda}\|_0 \\ \text{s.t.} \quad & \boldsymbol{\lambda} \in \mathcal{L}. \end{aligned} \tag{1}$$

Here, the objective minimizes the *logistic loss* $l(\boldsymbol{\lambda}) := \frac{1}{N} \sum_{i=1}^{N} \log(1 + \exp(-\langle \boldsymbol{\lambda}, y_i \boldsymbol{x}_i \rangle))$ for AUC and risk calibration, and penalizes the ℓ_0-norm $\|\boldsymbol{\lambda}\|_0 := \sum_{j=0}^{d} \mathbb{1}[\lambda_j \neq 0]$ for sparsity. The trade-off parameter C_0 controls the balance between these two objectives, and represents the maximum log-likelihood that RiskSlimMINLP will sacrifice to remove a feature from the optimal model[1] . The feasible region restricts coefficients to a small set of bounded integers such as $\mathcal{L} = \{-5, \ldots, 5\}^{d+1}$, and may be further customized to include any of the operational constraints in Table 1. RiskSlimMINLP is formulated to capture exact ob-

Constraint Type	**Example**
Feature Selection	Choose between 5 to 10 total features
Group Sparsity	Include either *male* or $female$ in the model but not both
Risk Stratification	Use at most 3 thresholds for age indicator variables: $\sum_{k=1}^{100} \mathbb{1}[age \leq k] \leq 3$
Logical Structure	If *male* is in model, then include *hypertension* or $bmi \geq 30$ as a control
Probability	Predict $\Pr(y = +1 \mid \boldsymbol{x}) \geq 0.90$ when *male* = TRUE and *hypertension* = TRUE

Table 1: Operational constraints that can be enforced on risk scores by including additional constraints in the feasible region of RiskSlimMINLP.

jectives and constraints for risk scores so that the optimal solution to RiskSlimMINLP corresponds to the model that attains the best possible performance among the class of models that satisfy constraints on model form. This statement deserves some qualification. In particular, an optimal solution to RiskSlimMINLP attains the lowest value of the logistic loss among the set of feasible models on the training data - provided that C_0 is small enough. Our empirical results in Section 6 show that models that minimize the logistic loss

1. When $\mathbf{0} \in \mathcal{L}$, we can bound the trade-off parameter to values such that $C_0 \in (0, \log(2))$. If $\mathbf{0} \in \mathcal{L}$, then setting $C_0 \geq \log(2)$ will provably return $\boldsymbol{\lambda}^* = \mathbf{0}$ as the optimal solution.

perform well in terms of AUC and risk calibration on the training data, and this performance typically generalizes to the test data given the simplicity of the model class. There are theoretical reasons to explain why minimizing the logistic loss results in good AUC and risk calibration. In particular, the logistic loss is a strictly proper loss function (Reid and Williamson, 2010) that yields well-calibrated estimates of predicted risk under the parametric assumption that the risk can be modeled using a logistic link function (see Menon et al., 2012, for a discussion). In addition, the work of Kotlowski et al. (2011) shows that a "balanced" version of the logistic loss forms a lower bound on 1 - AUC, which means that minimizing the logistic loss indirectly maximizes a surrogate of AUC (i.e., a lower bound on a scaled version of AUC).

Optimizing RiskSlimMINLP is a challenging computational task since MINLP problems are $\mathcal{NP}$-hard (Bonami et al., 2012), ℓ_0-regularization is $\mathcal{NP}$-hard (Amaldi and Kann, 1998), and minimizing over integers is $\mathcal{NP}$-hard (Gary and Johnson, 1979). These worst-case complexity results suggest that RiskSlimMINLP may be intractable for large dimensional datasets. As we show, however, RiskSlimMINLP can be solved to optimality for a range of real-world datasets in minutes, and in a way that scales linearly in N.

Assumptions, Notation and Terminology

We use the following notation. We denote the objective value function of RiskSlimMINLP as $V(\boldsymbol{\lambda}) := l(\boldsymbol{\lambda}) + C_0 \|\boldsymbol{\lambda}\|_0$, and denote an optimal solution as $\boldsymbol{\lambda}^* \in \operatorname{argmin}_{\boldsymbol{\lambda} \in \mathcal{L}} V(\boldsymbol{\lambda})$. We bound the values of objective value function and its components at the optimal solution $\boldsymbol{\lambda}^*$ as follows: $V(\boldsymbol{\lambda}^*) \in [V^{\min}, V^{\max}]$, $l(\boldsymbol{\lambda}^*) \in [L^{\min}, L^{\max}]$, $\|\boldsymbol{\lambda}^*\|_0 \in [R^{\min}, R^{\max}]$. In addition, we define the set of feasible values for each coefficient as $\lambda_j \in \mathcal{L}_j$ for $j = 0, \ldots, d$, and denote bounds as $\Lambda_j^{\min} = \min_{\boldsymbol{\lambda}_j \in \mathcal{L}_j} \lambda_j$ and $\Lambda_j^{\max} = \max_{\boldsymbol{\lambda}_j \in \mathcal{L}_j} \lambda_j$.

Unless otherwise specified, we make the following assumptions for clarity of exposition: (i) the coefficient set contains the null vector, $\mathbf{0} \in \mathcal{L}$; (ii) the intercept is never penalized, which means that the more precise version of the objective function in (1) is $V(\boldsymbol{\lambda}) := l(\boldsymbol{\lambda}) + C_0 \left\|\boldsymbol{\lambda}_{[1,d]}\right\|_0$ where $\boldsymbol{\lambda} = [\lambda_0, \boldsymbol{\lambda}_{[1,d]}]$. Here, the first assumption is to ensure that a generic formulation of RiskSlimMINLP is always feasible, and the second assumption ensure that the intercept term is not regularized.

Since RiskSlimMINLP is a non-convex optimization problem, we need to distinguish between finding the optimal solution to RiskSlimMINLP and proving that this solution is optimal. We say that we have *solved* RiskSlimMINLP *to optimality* if and only if we achieve both tasks. We can assess the optimality of any solution $\boldsymbol{\lambda}$ through its *optimality gap* $\frac{V(\boldsymbol{\lambda}) - V^{\min}}{V(\boldsymbol{\lambda})}$. The optimality gap associated with RiskSlimMINLP is defined by the best integer feasible solution, $\boldsymbol{\lambda} \in \mathcal{L}$ such that $V(\boldsymbol{\lambda}) = V^{\max}$, and computed as $\frac{V^{\max} - V^{\min}}{V^{\max}}$. A *certificate of optimality* for RiskSlimMINLP corresponds to an optimality gap of 0.0%.

3. Methodology

In this section, we introduce the cutting plane algorithm that we use to solve the risk score problem, RiskSlimMINLP. In Section 3.1, we discuss a simple cutting plane algorithm to highlight the benefits of solving RiskSlimMINLP with such algorithms, and to explain why many cutting plane algorithms stall on non-convex problems. In Section 3.2, we present a new cutting plane algorithm that does not stall on RiskSlimMINLP. In Section 3.3, we illustrate the real-world performance of both cutting plane algorithms as well as off-the-shelf MINLP solvers, by using all approaches to solve difficult instances of RiskSlimMINLP.

3.1 Cutting Plane Algorithms

We start by presenting a simple cutting plane algorithm to solve RiskSlimMINLP that we refer to as CPA (Algorithm 1). In what follows, we use CPA to discuss the major elements of cutting plane algorithms, explain their advantages for solving RiskSlimMINLP, and illustrate their stalling behavior for non-convex problems.

CPA recovers the optimal solution to RiskSlimMINLP by iteratively solving a mixed-integer programming (MIP) *surrogate problem* where the loss function $l(\boldsymbol{\lambda})$ is approximated using cutting planes. A *cutting plane* or *cut* to the loss function is a supporting hyperplane at a point $\boldsymbol{\lambda}^t \in \mathcal{L}$ with the form

$$\theta \geq l(\boldsymbol{\lambda}^t) + \langle \nabla l(\boldsymbol{\lambda}^t), \boldsymbol{\lambda} - \boldsymbol{\lambda}^t \rangle.$$

Here, $\theta \in \mathbb{R}_+$ is an auxiliary variable that represents the value of the approximate loss function, and $l(\boldsymbol{\lambda}^t) \in \mathbb{R}_+$ and $\nabla l(\boldsymbol{\lambda}^t) \in \mathbb{R}^d$ are *cut parameters* that represent the value and gradient of the loss function at the point $\boldsymbol{\lambda}^t$

$$l(\boldsymbol{\lambda}^t) = \frac{1}{N}\sum_{i=1}^{N} \log(1 + \exp(-\langle \boldsymbol{\lambda}^t, y_i \boldsymbol{x}_i \rangle)) \quad \nabla l(\boldsymbol{\lambda}^t) = \frac{1}{N}\sum_{i=1}^{N} \frac{-y_i \boldsymbol{x}_i}{1 + \exp(-\langle \boldsymbol{\lambda}^t, y_i \boldsymbol{x}_i \rangle)}. \tag{3}$$

Multiple cuts can be combined to build a piecewise linear approximation of the loss function as shown in Figure 2. We denote a collection of k cuts at the points $\boldsymbol{\lambda}^1, \ldots, \boldsymbol{\lambda}^k$ as

$$\mathcal{H}^k(\theta, \boldsymbol{\lambda}) = \left\{ \theta \geq l(\boldsymbol{\lambda}^t) + \langle \nabla l(\boldsymbol{\lambda}^t), \boldsymbol{\lambda} - \boldsymbol{\lambda}^t \rangle \right\}_{t=1}^{k}$$

and express the *cutting plane approximation* of the loss function as

$$\hat{l}^k(\boldsymbol{\lambda}) = \min_{\theta \in \mathbb{R}} \mathcal{H}^k(\theta, \boldsymbol{\lambda}) = \min_{\theta \in \mathbb{R}} \max_{t=1\ldots k} \theta \geq l(\boldsymbol{\lambda}^t) + \langle \nabla l(\boldsymbol{\lambda}^t), \boldsymbol{\lambda} - \boldsymbol{\lambda}^t \rangle.$$

On iteration k, CPA solves a surrogate problem RiskSlimMIP $\left(\mathcal{H}^k(\theta, \boldsymbol{\lambda})\right)$ that minimizes the approximate loss function $\hat{l}^k(\boldsymbol{\lambda})$ instead of the original loss function $l(\boldsymbol{\lambda})$. CPA uses the optimal solution to the surrogate problem $(\theta^k, \boldsymbol{\lambda}^k)$ in two ways: (i) it adds a cut at $\boldsymbol{\lambda}^k$ to improve the cutting plane approximation $\hat{l}^k(\boldsymbol{\lambda})$; and (ii) it updates bounds on optimal value of RiskSlimMINLP to check convergence. CPA constructs an upper bound using the best solution across all iterations

$$V^{\max} = \min_{t=1\ldots k} V\left(\boldsymbol{\lambda}^t\right),$$

Algorithm 1 Cutting Plane Algorithm (CPA)

Input

$(\boldsymbol{x}_i, y_i)_{i=1}^N$	training data
$\mathcal{L}$	constraint set for RiskSlimMINLP
C_0	ℓ_0 penalty parameter for RiskSlimMINLP
$\varepsilon \in [0, 1]$	maximum optimality gap for returned solution

Initialize

$k \leftarrow 0$	iteration counter
$V^{\min} \leftarrow 0$	lower bound to the optimal value of RiskSlimMINLP
$V^{\max} \leftarrow \infty$	upper bound to the optimal value of RiskSlimMINLP
$\varepsilon^0 \leftarrow 1$	initial optimality gap
$\mathcal{H}^0(\theta, \boldsymbol{\lambda}) \leftarrow \{\theta \geq 0\}$	collection of cuts to the loss function

while $\varepsilon^k \geq \varepsilon^{\text{stop}}$ **do**
  solve RiskSlimMIP $\left(\mathcal{H}^k(\theta, \boldsymbol{\lambda})\right)$ to optimality and store optimizers θ^k and $\boldsymbol{\lambda}^k$
  compute cut parameters $l(\boldsymbol{\lambda}^k)$ and $\nabla l(\boldsymbol{\lambda}^k)$
  $\mathcal{H}^{k+1}(\theta, \boldsymbol{\lambda}) \leftarrow \mathcal{H}^k(\theta, \boldsymbol{\lambda}) \cup \left\{\theta \geq l(\boldsymbol{\lambda}^k) + \langle \nabla l(\boldsymbol{\lambda}^k), \boldsymbol{\lambda} - \boldsymbol{\lambda}^k \rangle\right\}$ ▷ add cut
  $V^{\min} \leftarrow \theta^k + C_0 \left\|\boldsymbol{\lambda}^k\right\|_0$ ▷ lower bound is optimal value of RiskSlimMIP
  $V^k \leftarrow l(\boldsymbol{\lambda}^k) + C_0 \left\|\boldsymbol{\lambda}^k\right\|_0$
  if $V^k < V^{\max}$ **then**
    $V^{\max} \leftarrow V^k$ ▷ update upper bound
    $\boldsymbol{\lambda}^{\text{best}} \leftarrow \boldsymbol{\lambda}^k$ ▷ update incumbent solution
  end if
  $\varepsilon^k \leftarrow 1 - (V^{\min}/V^{\max})$ ▷ update optimality gap
  $k \leftarrow k + 1$
end while

Output: $\boldsymbol{\lambda}^{\text{best}}$, ε-optimal solution to RiskSlimMINLP.

RiskSlimMIP $\left(\mathcal{H}^k(\theta, \boldsymbol{\lambda})\right)$ is a MIP surrogate of RiskSlimMINLP that minimizes a cutting-plane approximation of the loss function built using $\mathcal{H}^k(\theta, \boldsymbol{\lambda})$:

$$\begin{aligned} \min_{\theta, \boldsymbol{\lambda}} \quad & \theta + C_0 \left\|\boldsymbol{\lambda}\right\|_0 \\ \text{s.t.} \quad & \theta \in \mathcal{H}^k(\theta, \boldsymbol{\lambda}), \\ & \boldsymbol{\lambda} \in \mathcal{L}. \end{aligned} \tag{2}$$

We denote the optimizers of RiskSlimMIP $\left(\mathcal{H}^k(\theta, \boldsymbol{\lambda})\right)$ as $(\theta^k, \boldsymbol{\lambda}^k)$. We include a MIP formulation for RiskSlimMIP in Appendix B.

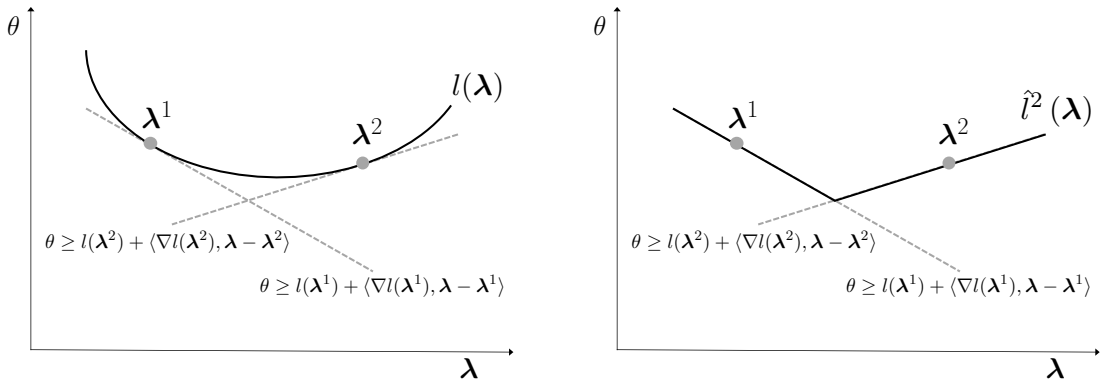

Figure 2: Cutting plane algorithms such as CPA build a piecewise linear approximation of the loss function using a collection of cutting planes (i.e., cuts). The plot on the left shows the loss function $l(\boldsymbol{\lambda})$ with cuts at the points $\boldsymbol{\lambda}^1$ and $\boldsymbol{\lambda}^2$. The plot on the right shows the approximate loss function $\hat{l}^2(\boldsymbol{\lambda}) = \min_\theta \mathcal{H}^2(\theta, \boldsymbol{\lambda})$ where $\mathcal{H}^2(\theta, \boldsymbol{\lambda})\{\theta \geq l(\boldsymbol{\lambda}^t) + \langle \nabla l(\boldsymbol{\lambda}^t), \boldsymbol{\lambda} - \boldsymbol{\lambda}^t \rangle\}_{t=1}^2$. Since the loss function is convex, it follows that $\hat{l}^k(\boldsymbol{\lambda}) \leq l(\boldsymbol{\lambda})$ for all $k \in \mathbb{N}$ and $\boldsymbol{\lambda} \in \mathcal{L}$.

and constructs a lower bound using the optimal solution from the most recent iteration as

$$V^{\min} = \theta^k + C_0 \|\boldsymbol{\lambda}^k\|_0.$$

To see that $V^{\min} \leq V(\boldsymbol{\lambda}^*)$, note that $\hat{l}^k(\boldsymbol{\lambda}) \leq l(\boldsymbol{\lambda})$ for all $\boldsymbol{\lambda} \in \mathcal{L}$ and $k \in \mathbb{N}$ (since a convex loss function is always underestimated by its cutting plane approximation, as depicted in Figure 2). In particular, for $\boldsymbol{\lambda}^* \in \operatorname{argmin}_{\boldsymbol{\lambda} \in \mathcal{L}} V(\boldsymbol{\lambda})$, we have

$$\hat{l}^k(\boldsymbol{\lambda}^*) + C_0 \|\boldsymbol{\lambda}^*\|_0 \leq l(\boldsymbol{\lambda}^*) + C_0 \|\boldsymbol{\lambda}^*\|_0 = V(\boldsymbol{\lambda}^*).$$

Since CPA picks $\boldsymbol{\lambda}^k$ as the minimizer of $\hat{l}^k(\boldsymbol{\lambda}) + C_0 \|\boldsymbol{\lambda}\|_0$, it then follows that

$$\theta^k + C_0 \|\boldsymbol{\lambda}^k\|_0 = \hat{l}^k\left(\boldsymbol{\lambda}^k\right) + C_0 \|\boldsymbol{\lambda}^k\|_0 \leq \hat{l}^k(\boldsymbol{\lambda}^*) + C_0 \|\boldsymbol{\lambda}^*\|_0 \leq V(\boldsymbol{\lambda}^*).$$

CPA converges to ε-optimal solution of RiskSlimMINLP after a finite number of iterations (see Kelley, 1960, for a proof). To see this, note that the cutting plane approximation of a convex loss function improves monotonically with each additional cut

$$\hat{l}^k(\boldsymbol{\lambda}) \leq \hat{l}^{k+m}(\boldsymbol{\lambda}) \leq l(\boldsymbol{\lambda}) \text{ for all } k, m \in \mathbb{N} \text{ and } \boldsymbol{\lambda} \in \mathcal{L}. \tag{4}$$

Since the cuts added at each iteration are not redundant, the lower bound $V^{\min}$ improves monotonically with each iteration. Once the CPA optimality gap $\varepsilon^k = 1 - V^{\min}/V^{\min}$ is less than a user threshold $\varepsilon^{\text{stop}}$, CPA terminates and returns a solution $\boldsymbol{\lambda}^{\text{best}}$ that provably belongs to the ε-level set of optimizers to RiskSlimMINLP.

Benefits of Solving RiskSlimMINLP with a Cutting Plane Algorithm

CPA illustrates two key benefits of cutting plane algorithms for general risk minimization problems (Joachims, 2006; Teo et al., 2007; Franc and Sonnenburg, 2008): scalability in

the sample size and control over data-related computation. Both benefits arise from the fact that cutting plane algorithms use training data to compute cut parameters in a single isolated step (see Step 3 in Algorithm 1). Since cut parameters can be computed using elementary matrix-vector operations in $O(Nd)$ time at each iteration, the running time for the entire algorithm scales linearly in N for fixed d (see Figure 3.1). Moreover, this setup lets users further reduce data-related computation by using custom implementations that parallelize computation, or exploiting properties of the model class (see e.g., Section 5).

CPA also illustrates a unique benefit of using cutting plane algorithm for the risk score problem. Specifically, CPA recovers the optimal solution of a nonlinear problem RiskSlim-MINLP by iteratively solving the linearized surrogate RiskSlimMIP. In practice, this means that we can fit risk scores with a MIP solver instead of a MINLP solver. As we show in Section 3.3, this can substantially improve our ability to solve RiskSlimMINLP since MIP solvers typically exhibit better off-the-shelf performance than MINLP solvers (due to fact that MINLP solvers are designed to handle a diverse set of optimization problems).

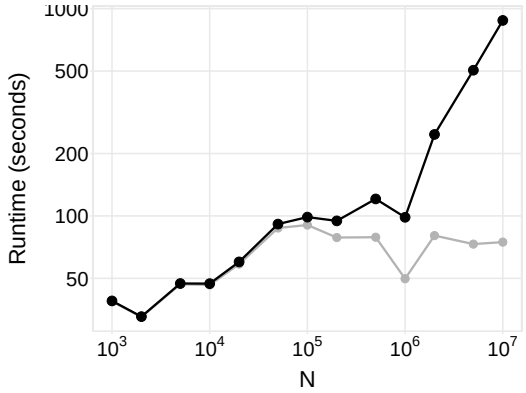

Figure 3: Runtime of CPA on simulated datasets with $d = 10$ dimensions and $N \in [10^3, 10^8]$ samples (see Appendix C). As N increases, solver time (grey) remains roughly constant. The total runtime (black) scales at $O(N)$, which reflects the additional time needed to compute cut parameters for datasets with large sample sizes.

Stalling Behavior of Cutting Plane Algorithms on Non-Convex Problems

Many cutting plane algorithms used to solve for large-scale risk minimization problems (see e.g., Joachims, 2006; Franc and Sonnenburg, 2008; Teo et al., 2009) are similar to CPA in that they solve a surrogate optimization problem at each iteration (see Step 5 of Algorithm 1). When these algorithms are used to solve a convex optimization problem, the surrogate problem is convex and tractable. When these algorithms are applied to non-convex problems, however, the surrogate problem is non-convex and may be intractable. In practice, this leads such algorithms to solve surrogate problems that require an unreasonable amount of time to solve to optimality. We refer to this behavior as *stalling*.

In Figure 4, we illustrate the stalling behavior for CPA. Here, the first few iterations are quick since RiskSlimMIP $\left(\mathcal{H}^k(\theta, \boldsymbol{\lambda})\right)$ can easily solved to optimality when it contains a trivial approximation of the loss function. However, RiskSlimMIP $\left(\mathcal{H}^k(\theta, \boldsymbol{\lambda})\right)$ becomes

increasingly difficult to optimize as the approximate loss function improves with each iteration. On the $d = 10$ instance, CPA does not stall as the MIP solver is powerful enough to solve the surrogate problem RiskSlimMIP $\left(\mathcal{H}^k(\theta, \boldsymbol{\lambda})\right)$ at all iterations. On the $d = 20$ instance, however, the time to solve RiskSlimMIP $\left(\mathcal{H}^k(\theta, \boldsymbol{\lambda})\right)$ increases exponentially and CPA eventually stalls at iteration $k = 86$. In this case, the best feasible solution returned by CPA has a large optimality gap, and corresponds to a risk score model with poor performance (which we would expect as it was fit by optimizing a surrogate problem with a poor approximation of the original loss function).

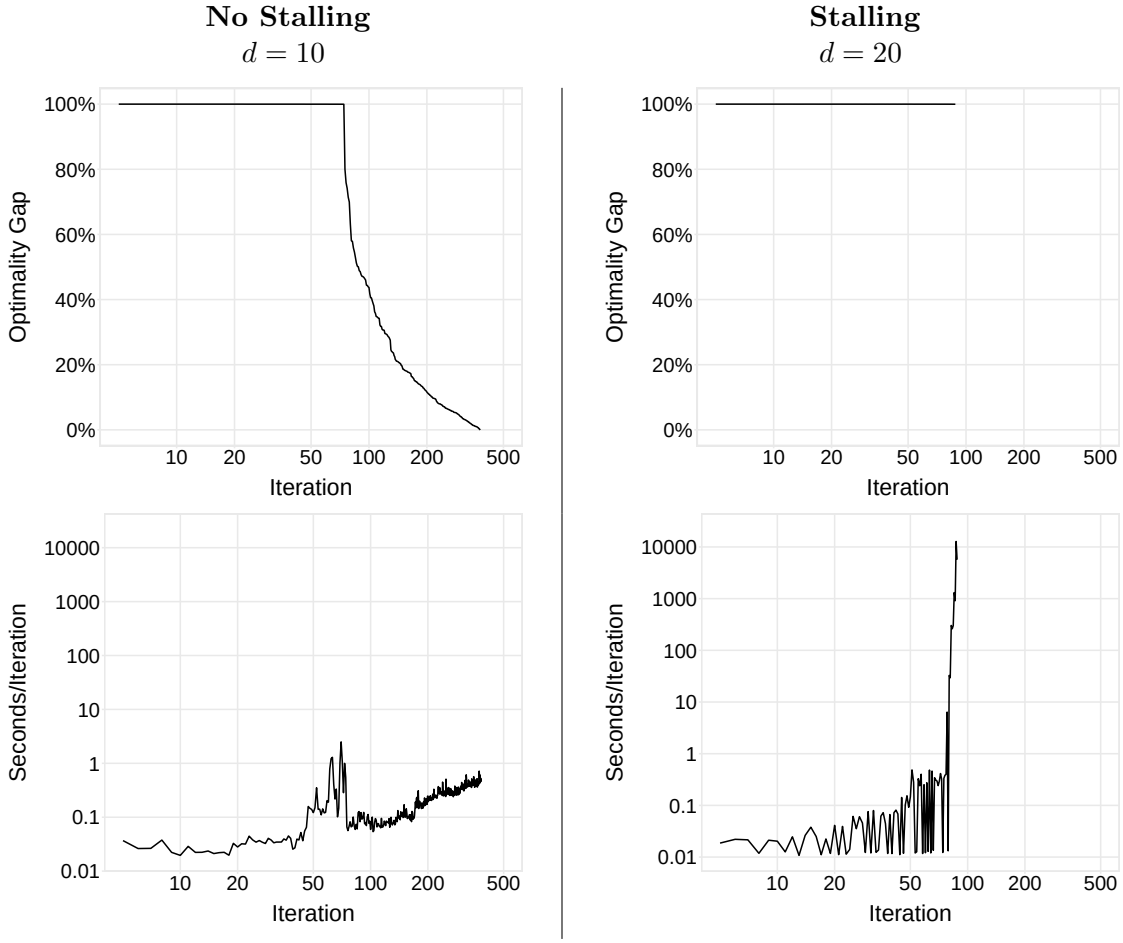

Figure 4: Performance of CPA when solving RiskSlimMINLP instances for simulated datasets with $d = 10$ (left) and $d = 20$ (right) and $N = 50$'000 (see Appendix C). We show the optimality gap (top) and time per iteration (bottom, in log-scale) for each iteration over 6 hours. CPA quickly solves the $d = 10$ instance, but stalls on the $d = 20$ instance as the time to solve RiskSlimMIP to optimality increases exponentially starting at iteration 86. In this case, the best solution found after 6 hours is a risk score with poor performance.

There is no easy fix to prevent cutting plane algorithms such as CPA from stalling on non-convex problems. This is because these algorithms are designed in a way that requires a provably optimal solution at each iteration to compute a valid lower bound and

check convergence. In a non-convex setting, this means finding an optimal solution at each iteration, but pairing this solution with an optimality gap of 0.0%. If, for example, CPA only solved RiskSlimMIP $\left(\mathcal{H}^k(\theta, \boldsymbol{\lambda})\right)$ at a feasible solution with a non-zero optimality gap, then the resulting lower bound could exceed the true optimal value, leading the algorithm to terminate early and return suboptimal solution with invalid bounds.

Seeing how stalling is related to the mechanism used to check convergence, an alternative (but flawed) approach is use a cutting plane algorithm that add cuts at central points of RiskSlimMIP $\left(\mathcal{H}^k(\theta, \boldsymbol{\lambda})\right)$ as these algorithms can guarantee convergence in a fixed number of iterations through a spatial argument (e.g., the center of gravity of Levin 1965 or the analytic center of Atkinson and Vaidya 1995; Goffin and Vial 2002). In this case, however, stalling would still occur because we would still have to solve a non-convex optimization problem at each iteration to compute central points.

3.2 Lattice Cutting Plane Algorithm

To avoid the stalling of cutting-plane algorithms on non-convex optimization problems, we solve RiskSlimMINLP with the *lattice cutting plane algorithm* (LCPA; Algorithm 2).

LCPA finds a globally optimal solution to RiskSlimMINLP by using a simultaneous approach that: (i) solves the surrogate problem RiskSlimMIP $(\mathcal{H}(\theta, \boldsymbol{\lambda}))$ by building a single branch-and-bound tree; and (ii) dynamically updates the cutting plane approximation used in the surrogate problem with adds cuts at integer feasible solutions. In practice, LCPA can be implemented with a modern MIP solver, which efficiently handles branch-and-bound search and provides *control callbacks* that allow users to intervene and add cuts.

As shown in Figure 5, LCPA does not stall because it does not have to solve a non-convex optimization problem to optimality between cuts. However, it retains the key benefits of cutting plane algorithms, namely: (i) the ability to use a MIP solver (since it does not directly minimize the nonlinear loss function); (ii) scalability in the sample size (since training data is only used to compute cut parameters); and (iii) control over data-related computation (since cut parameters can still be computed with a customized implementation).

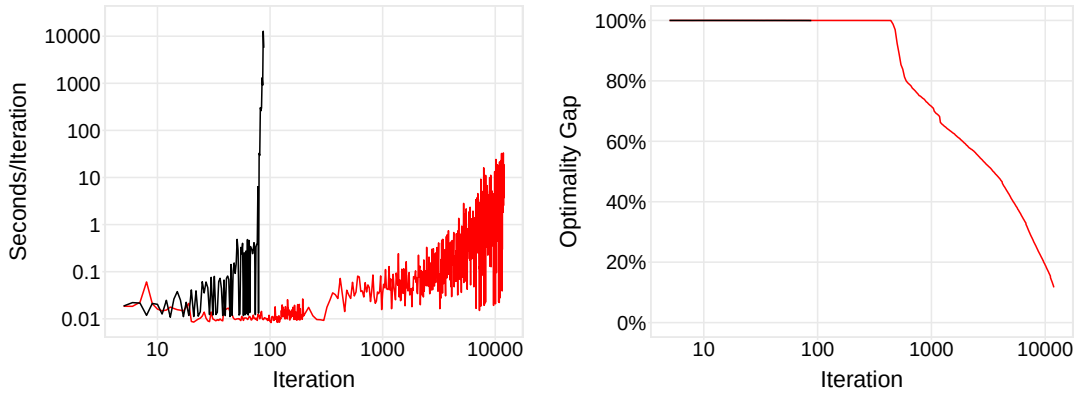

Figure 5: Performance of LCPA (red) and CPA (black) when solving the RiskSlimMINLP instance from Figure 4. Unlike CPA, LCPA does not stall and proceeds to solve RiskSlimMINLP to obtain a high quality risk score with a small optimality gap.

In what follows, we describe the key elements of Algorithm 2 in greater detail.

- **Surrogate LP**: LCPA recovers the solution to RiskSlimMINLP by repeatedly solving a surrogate linear program (LP) RiskSlimLP $(\mathcal{H}(\theta, \boldsymbol{\lambda}), \mathcal{P})$ over the branch-and-bound search process. This is a convex relaxation of RiskSlimMIP $(\mathcal{H}(\theta, \boldsymbol{\lambda}))$ whose feasible region is restricted to *partition* of the convex hull of the original feasible region $\mathcal{P} \subseteq \text{conv}(\mathcal{L})$.

- **Branch-and-Bound**: In Algorithm 2, the branch-and-bound search is carried out by solving *nodes* within a collection of nodes $\mathcal{T}$. Here, each node $(\mathcal{P}, V)$ consists of a partition $\mathcal{P}$ and a lower bound of the optimal objective value of the surrogate LP for V. The partitions of all nodes in $\mathcal{T}$ are disjoint. At each iteration, LCPA removes a node $(\mathcal{P}^r, V^r)$ from the $\mathcal{T}$ using NodeSelectionRule in Step 2 and solves RiskSlimLP $(\mathcal{H}(\theta, \boldsymbol{\lambda}), \mathcal{P}^r)$ in Step 3. This results in one of three outcomes, based on the solution to RiskSlimLP $(\mathcal{H}(\theta, \boldsymbol{\lambda}), \mathcal{P}^r)$:

  1. If RiskSlimLP $(\mathcal{H}(\theta, \boldsymbol{\lambda}), \mathcal{P}^r)$ is infeasible, the node is discarded.
  2. If RiskSlimLP $(\mathcal{H}(\theta, \boldsymbol{\lambda}), \mathcal{P}^r)$ yields a solution that is integer feasible $\boldsymbol{\lambda}^r \in \mathcal{L}$, and a cut is added at $\boldsymbol{\lambda}^r$ (Step 5).
  3. If RiskSlimLP $(\mathcal{H}(\theta, \boldsymbol{\lambda}), \mathcal{P}^r)$ yields a solution that is not integer feasible $\boldsymbol{\lambda}^r \notin \mathcal{L}$, then the outcome depends on the optimal objective value V^r. If $V^r \geq V^{\max}$ then it is discarded, as it cannot yield an integer feasible solution that has objective value $V^{\max}$. If $\mathcal{P}^r \leq V^{\max}$, then two new child nodes are added to the pool $\mathcal{T}$ in Step 16, namely $(V^r, \mathcal{P}^{\text{I}})$ and $(V^r, \mathcal{P}^{\text{II}})$.

- **Bounds**: LCPA checks convergence by computing bounds on the optimal objective value $V(\boldsymbol{\lambda}^*)$. The upper bound is computed in the same way as CPA – by using the best feasible solution as $V^{\max} = V\left(\boldsymbol{\lambda}^{\text{best}}\right)$ (Step 10). The lower bound is computed using the smallest objective value of RiskSlimLP from all active nodes in Step 18. This quantity represents the objective value of the surrogate problem RiskSlimLP $\left(\mathcal{H}^k(\theta, \boldsymbol{\lambda}), \bigcup_s \mathcal{P}^s\right)$ over the remaining search region $\bigcup_s \mathcal{P}^s$.

- **Convergence**: As LCPA processes nodes with each iteration, it discovers an increasing number of integer feasible solutions, $V^{\max}$ decreases monotonically until the optimal solution is found. In addition, the effective search region $\bigcup_s .\mathcal{P}^s$, which ensures that the lower bound $V^{\min}$ increases monotonically. Since there are a finite number of nodes, LCPA terminates after a finite number of iterations (see Remark 1). LCPA returns an optimal solution to RiskSlimMINLP as long as cuts are added at any solution where LCPA updates the incumbent (Step 10).

Remark 1 (Convergence of Lattice Cutting Plane Algorithm)
For any training dataset $(\boldsymbol{x}_i, y_i)_{i=1}^N$, any trade-off parameter $C_0 \geq 0$, and any finite coefficient set $\mathcal{L} \subseteq \mathbb{Z}^{d+1}$, the lattice cutting plane algorithm (Algorithm 2) returns an optimal solution to the risk score problem RiskSlimMINLP *after computing at most $|\mathcal{L}|$ cutting planes and processing at most $2^{D(\mathcal{L})} - 1$ nodes. Here:*

$$D(\mathcal{L}) = \prod_{j=0}^{d} (\Lambda_j^{max} - \Lambda_j^{min} + 1).$$

We make the following observations regarding LCPA:

- For a fixed collection of cutting planes, the lower bound from LCPA is weaker than the lower bound from CPA. Explicitly, CPA constructs a lower bound using an integer feasible solution as $V^{\min} = \text{argmin}_{\boldsymbol{\lambda} \in \mathcal{L}} \hat{l}^k(\boldsymbol{\lambda}) + C_0 \|\boldsymbol{\lambda}\|_0$. In contrast, LCPA constructs a lower bound using a solution that is not necessarily integer feasible. Thus, on instances where it does not stall, CPA may converge faster than the LCPA since it produces a stronger lower bound at each iteration.

- Since LCPA adds cuts at feasible solutions, and that the solution quality is affected by the fidelity of the approximation loss function, LCPA may initially find integer feasible solutions that correspond to poor models. To mitigate this issue, we initialize LCPA with an initial set of cutting planes in our initialization procedure in Section 4.2.2. This also improves the lower bound estimates produced by LCPA, given that the optimal solution to the cutting plane approximation of the loss function is part of the lower bound estimate.

- LCPA is easy to implement. Modern MIP solvers provide a efficient an implementation of branch-and-bound as well as options for NodeSelectionRule and PartitionSplittingRule. Users can intervene within the branch-and-bound search using *control callbacks*. In our implementation, which uses CPLEX 12.6, we use a *LazyCutCallback* to intervene when the branch-and-bound finds an integer feasible solution after Step 5, which we then use to add cuts in Step 7. We also use a *HeuristicCallback* to periodically run rounding and polishing heuristics (Section 4.1) as well as the chained updates procedure (Section 4.2.1). In theory, we could also use callbacks to intervene at the node-level to speed up convergence by, for instance, adding cuts at solutions that are not integer feasible in Step 14. In practice, however, this approach substantially slows down LCPA due to the overhead in using a callback at every node (note that even small instances of RiskSlimMINLP require processing a very large number of nodes).

Algorithm 2 Lattice Cutting Plane Algorithm (LCPA)

Input

$(\boldsymbol{x}_i, y_i)_{i=1}^N$	training data
$\mathcal{L}$	constraint set for RiskSlimMINLP
C_0	ℓ_0 penalty parameter for RiskSlimMINLP
$\varepsilon \in [0, 1]$	maximum optimality gap for returned solution
NodeSelectionRule	provided by MIP solver
PartitionSplittingRule	provided by MIP solver

Initialize

$(V^{\min}, V^{\max}) \leftarrow (0, \infty)$	bounds on the optimal value of RiskSlimMINLP
$\mathcal{H}^0(\theta, \boldsymbol{\lambda}) \leftarrow \{\theta \geq 0\}$	collection of cuts to the loss function
$\mathcal{P}^0 \leftarrow \text{conv}(\mathcal{L})$	partition for root node
$V^0 \leftarrow V^{\min}$	lower bound for root node
$\mathcal{T} \leftarrow \{(\mathcal{P}^0, V^0)\}$	set of nodes in branch-and-bound tree

while $\frac{V^{\max} - V^{\min}}{V^{\max}} > \varepsilon$ **do**
  pick and remove $(\mathcal{P}^r, V^r)$ from $\mathcal{T}$ using NodeSelectionRule
  solve RiskSlimLP $\left(\mathcal{H}^k(\theta, \boldsymbol{\lambda}), \mathcal{P}^r\right)$ to obtain optimizers $(\theta^r, \boldsymbol{\lambda}^r)$ ▷ if infeasible, go to Step 2
  $V \leftarrow \theta^r + C_0 \left\|\boldsymbol{\lambda}^r\right\|_0$
  if $\boldsymbol{\lambda}^r \in \mathcal{L}$ **then** ▷ optional: polish $\boldsymbol{\lambda}^r$ via DCD (Alg. 3)
    compute cut parameters, $l(\boldsymbol{\lambda}^r)$ and $\nabla l(\boldsymbol{\lambda}^r)$
    $\mathcal{H}^{k+1}(\theta, \boldsymbol{\lambda}) \leftarrow \mathcal{H}^k(\theta, \boldsymbol{\lambda}) \cup \{\theta \geq l(\boldsymbol{\lambda}^r) + \langle \nabla l(\boldsymbol{\lambda}^r), \boldsymbol{\lambda} - \boldsymbol{\lambda}^r \rangle\}$ ▷ add cut
    $k \leftarrow k + 1$
    if $V < V^{\max}$ **then**
      $\boldsymbol{\lambda}^{\text{best}} \leftarrow \boldsymbol{\lambda}^r$ ▷ update incumbent solution
      $V^{\max} \leftarrow V$ ▷ optional: improve bounds via chained updates (Alg. 5)
      $\mathcal{T} \leftarrow \mathcal{T} \setminus \{(\mathcal{P}^s, V^s) \mid V^s \geq V^{\max}\}$ ▷ prune nodes that are provably suboptimal
    end if
  else
    split $\mathcal{P}^r$ into $\mathcal{P}'$ and $\mathcal{P}''$ using PartitionSplittingRule
    add $(\mathcal{P}', V)$ and $\mathcal{P}'', V)$ to $\mathcal{T}$
    if $V > V^{\min}$ **then**
      $V^{\min} \leftarrow V$ ▷ optional: improve bounds via chained updates (Alg. 5)
    end if
  end if
end while

Output: $\boldsymbol{\lambda}^{\text{best}}$, ε-optimal solution to RiskSlimMINLP

RiskSlimLP $(\mathcal{H}(\theta, \boldsymbol{\lambda}), \mathcal{P})$ is an LP relaxation of RiskSlimMIP $(\mathcal{H}(\theta, \boldsymbol{\lambda}))$ over the partition $\mathcal{P} \subseteq \text{conv}(\mathcal{L})$:

$$\begin{aligned} \min_{\theta, \boldsymbol{\lambda}, \boldsymbol{\alpha}} \quad & \theta + C_0 \sum_{j=1}^{d} \alpha_j \\ \text{s.t.} \quad & \theta \in \mathcal{H}(\theta, \boldsymbol{\lambda}) \\ & \boldsymbol{\lambda} \in \mathcal{P} \\ & \alpha_j = \max(\lambda_j, 0)/\Lambda_j^{\max} + \min(\lambda_j, 0)/\Lambda_j^{\min} \text{ for } j = 1, \ldots, d \end{aligned} \tag{5}$$

We include an LP formulation for RiskSlimLP in Appendix B.

3.3 Empirical Performance of Algorithms to Solve the Risk Score Problem

To illustrate the performance of both cutting plane algorithms, we used each algorithm to solve difficult instances of RiskSlimMINLP on simulated datasets with varying dimensions d and sample sizes N (see Appendix C). As a baseline, we solved the same instances using 3 MINLP algorithms[2] in a commercial MINLP solver[3].

In Figure 6, we compare all methods in terms of the following performance metrics:

- *time to find a near-optimal solution*, meaning a solution within 10% of the optimal value but without a proof of optimality. This measures the time needed to obtain a solution with low loss, which corresponds to a risk score with good AUC and risk calibration.
- *optimality gap of best solution at termination*, which is 0.0% if and only if the method finds the optimal solution *and* provides the proof of optimality within a 6 hour time limit.
- *% of time spent on data-related computation*, meaning the time spent evaluating the value, gradient, or Hessian of the loss function.

As shown, a basic implementation of LCPA[4] can find the optimal solution to RiskSlimMINLP for almost all instances, and pair this solution with a small optimality gap in almost all cases. In contrast, CPA can only provide the same level of performance on limited low-dimensional instances, given that it stalls on instances with $d \geq 15$. On such instances, CPA stalls after a few iterations and returns a risk score that performs poorly (which makes sense since the best solution found optimizes a poor approximation of the loss function with few cuts).

In this case, our results show that the MINLP solver could only handle instances of RiskSlimMINLP for datasets with limited sample sizes and/or dimensions. On larger instances, the solver fails to converge in the 6-hour time limit, and also fails to find a high quality feasible solution. Here, the MINLP solver spend the majority of its time dealing with operations that involve data-related computation. Seeing how a MINLP solver is designed to solve a diverse set of optimization problems, it is unlikely that it can identify and exploit the structure of the risk score problem in the same way as the cutting plane algorithms.

2. Since all 3 MINLP algorithms behave similarly, we only show the best performing in Figure 6 and include results for the remaining MINLP algorithms in Appendix C.
3. There exist several off-the-shelf MINLP solvers (see Bussieck and Vigerske, 2010, for a list). We used Artelsys Knitro 9.0, which is an updated version of the MINLP solver from Byrd et al. (2006), because it let us: (i) control data-related computation, by letting us write our own function handles for the objective, its gradient and Hessian; and (ii) solve LP subproblems using CPLEX, which is the same solver that we used for our algorithms.
4. The performance reflects a basic implementation of LCPA on a difficult instance of RiskSlimMINLP. We improve the performance of LCPA with regards to all metrics in Sections 4 and 5.

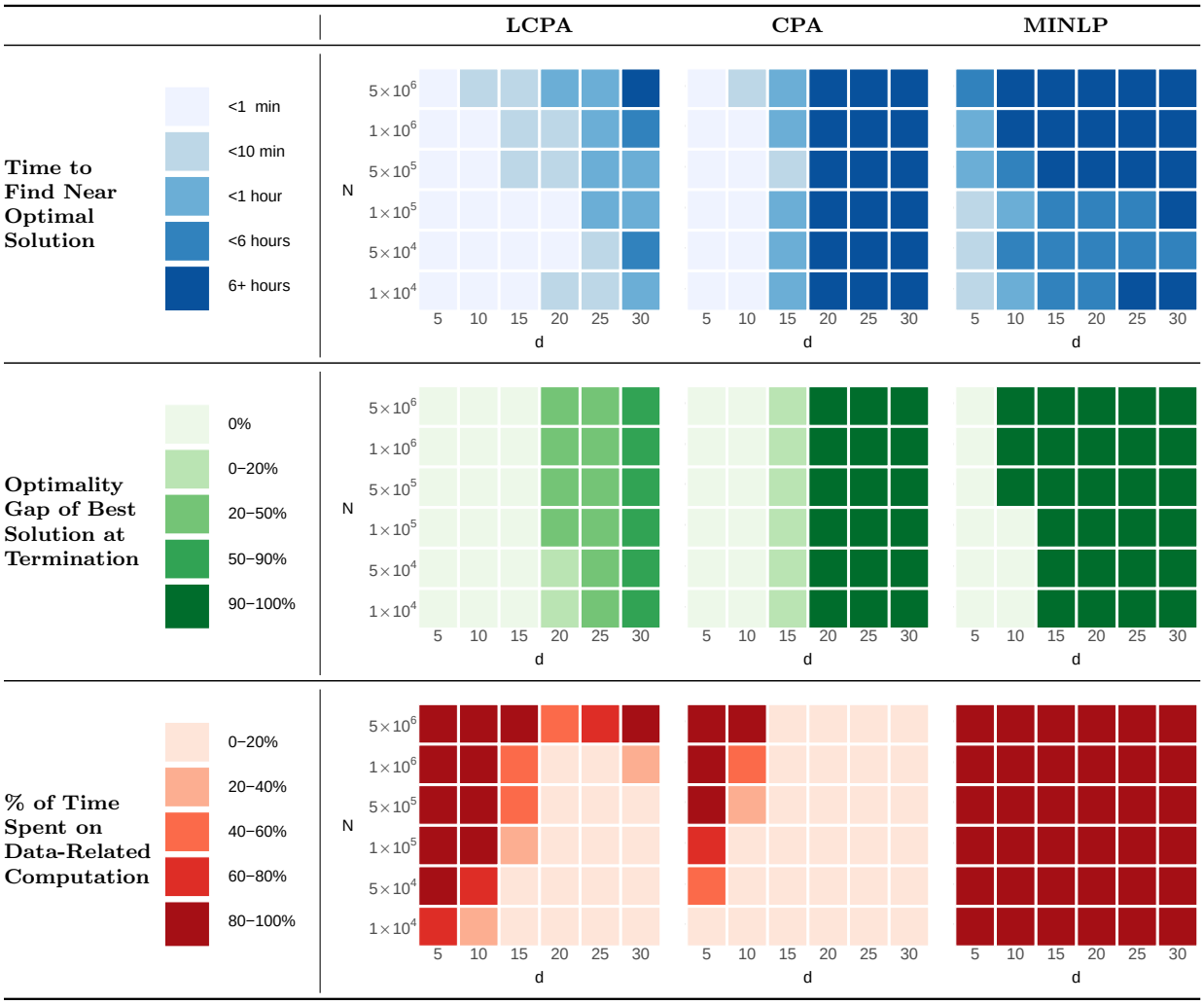

Figure 6: Performance of algorithms on hard RiskSlimMINLP instances for simulated datasets with varying dimensions d and sample sizes N (see Appendix C). MINLP fails on instances with large d or N as it spends a large amount of time on data-related computation. In comparison, CPA and LCPA scale linearly in N – that is, if they can solve an instance for fixed d, then they can solve instances for larger N in $O(N)$ time. CPA stalls on all instances when $d \geq 15$, returning highly suboptimal solutions when $d \geq 20$. In contrast, LCPA does not stall on any instances, and recovers a near optimal solution in all cases, pairing solutions with optimality gaps that range between 0.0 - 62.2% depending on d. Results reflect performance for a basic LCPA implementation without the improvements in Sections 4 and 5, and a Active Set MINLP algorithm (see Appendix C for additional MINLP algorithms).

4. Algorithmic Improvements

In this section, we present several techniques to improve the performance of the lattice cutting plane algorithm (LCPA) on the risk score problem (RiskSlimMINLP).

4.1 Generating High Quality Feasible Solutions

In what follows, we present two techniques to generate and polish integer feasible solutions for RiskSlimMINLP. We use these techniques in LCPA to improve integer feasible solutions found by the MIP solver, and to round continuous solutions to RiskSlimLP. In addition, we use these techniques to design improved heuristic methods to learn risk scores from data in Section 6.

4.1.1 Discrete Coordinate Descent

Discrete coordinate descent (DCD) is a technique for polishing integer feasible solutions (Algorithm 3). It takes as input an integer feasible solution $\boldsymbol{\lambda} = (\lambda_0, \ldots, \lambda_d) \in \mathcal{L}$ and iteratively moves along a single dimension j to attain an integer feasible solution with a lower objective value. The descent direction at each iteration is chosen in a greedy way, as the dimension that minimizes the objective value $j \in \operatorname{argmin} V(\boldsymbol{\lambda} + \delta_j e_j)$.

DCD terminates once it can no longer strictly improve the the objective value. This rules out the possibility of cycling, and thereby ensures that it terminates after a finite number of iterations. The polished solution satisfies a type of local optimality guarantee for the discrete setting: namely, the solution is *1-opt* with respect to the objective, meaning that the objective will not improve along any single dimension (see e.g., Park and Boyd, 2015b, for a technique to find a 1-opt point for a different discrete optimization problem).

In practice, the most expensive part of DCD involves determining a step-size $\delta_j \in \Delta_j$ that minimizes the objective in dimension j (Step 4 of Algorithm 3). The computation for this step can be significantly reduced by using a bisection search algorithm that exploits the convexity of the loss function, to reduce the number of loss function evaluations. This approach requires a total of $\log_2(|\mathcal{L}_j|)Nd$ flops per iteration, which is an improvement over the $(|\mathcal{L}_j| - 1)Nd$ flops per iteration required from the naive exhaustive search strategy (i.e., where we evaluate the loss for all $(|\mathcal{L}_j| - 1)$ values of λ_j other than current value).

In Figure 4.1.1, we show how DCD can improve the performance of LCPA when we use it to polish feasible solutions found by the MIP solver (i.e., in Step 5 of Algorithm 2).

Algorithm 3 Discrete Coordinate Descent (DCD)

Input

$(\boldsymbol{x}_i, y_i)_{i=1}^N$ — training data
$\mathcal{L}$ — constraint set for RiskSlimMINLP
C_0 — ℓ_0 penalty parameter for RiskSlimMINLP
$\boldsymbol{\lambda} \in \mathcal{L}$ — integer feasible solution to RiskSlimMINLP

Initialize

$V \leftarrow V(\boldsymbol{\lambda})$ — objective value at current solution
$\mathcal{J} \leftarrow \{0, \ldots, d\}$ — valid search dimensions

repeat
  for $j \in \mathcal{J}$ **do**
    $\Delta_j \leftarrow \{\delta \in \mathbb{Z} \mid \boldsymbol{\lambda} + \delta e_j \in \mathcal{L}\}$ ▷ list feasible moves along dim j
    $\delta_j \leftarrow \text{argmin}_{\delta \in \Delta_j} V(\boldsymbol{\lambda} + \delta)$ ▷ find best move along dim j
    $v_j \leftarrow V(\boldsymbol{\lambda} + \delta_j e_j)$ ▷ store objective value for best move along dim j
  end for
  $m \leftarrow \text{argmin}_{j \in \mathcal{J}} v_j$ ▷ find descent dimension
  if $v_m < V$ **then**
    $V \leftarrow v_m$
    $\boldsymbol{\lambda} \leftarrow \boldsymbol{\lambda} + \delta_m e_m$
    $\mathcal{J} \leftarrow \{0, \ldots, d\} \setminus \{m\}$ ▷ ignore dim m on next iteration
  end if
until $v_m \geq V$

Output: $\boldsymbol{\lambda}$, solution that is 1-opt with respect to the objective of RiskSlimMINLP

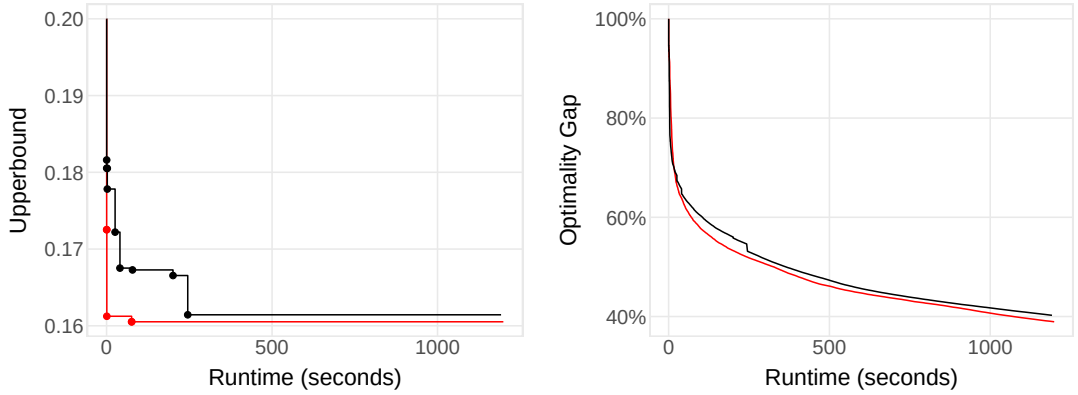

Figure 7: Performance of LCPA with DCD (red) and without DCD (black). We use DCD to polish every integer feasible solution found by the MIP solver whose objective value is within 10% of the current upper bound. We plot large points to show when LCPA updates the incumbent solution. Results reflect performance on RiskSlimMINLP for a simulated dataset with $d = 30$ and $N = 50$'000 (see Appendix C).

4.1.2 Sequential Rounding

Sequential rounding (Algorithm 4) is a technique to round continuous solutions in a way that accounts for objective of RiskSlimMINLP. Given a continuous solution $\boldsymbol{\lambda}^{\text{cts}} \in \text{conv}(\mathcal{L})$, the technique rounds one component at a time, either up or down, in a way that minimizes the objective value of RiskSlimMINLP.

On step k, the technique has already rounded k components, and needs to round one of the remaining $d-k$ components to either $\lceil \lambda_j^{\text{cts}} \rceil$ or $\lfloor \lambda_j^{\text{cts}} \rfloor$. To this end, it computes the objective value of each feasible component/direction pair, and chooses the best one. This requires $\sum_{i=1}^{i=d-k} 2i = (d-k)(d-k+1)$ evaluations of the loss function on Step k, meaning that the technique terminates after $\frac{1}{3}d(d^2-1)$ evaluations of the loss function.

In Figure 4.1.2, we show the impact of using sequential rounding in LCPA to round the continuous solution to RiskSlimLP whenever the lower bound is updated (i.e., Step 3 of Algorithm 2). We then polish the rounded solution via DCD to increase the likelihood that it will update the incumbent solution. As shown, this strategy reduces the time needed for LCPA to produce a higher quality risk score, and attain a lower optimality gap.

Algorithm 4 Sequential Rounding (SR)

Input

$(\boldsymbol{x}_i, y_i)_{i=1}^N$	training data
$\mathcal{L}$	constraint set for RiskSlimMINLP
C_0	ℓ_0 penalty parameter for RiskSlimMINLP
$\boldsymbol{\lambda} \in \text{conv}(\mathcal{L})$	feasible solution to RiskSlimLP

Initialize

$\mathcal{J}^{\text{cts}} \leftarrow \{0, \dots d\}$ index set of features that need to be rounded

while $\mathcal{J}^{\text{cts}} \neq \varnothing$ **do**
  $\boldsymbol{\lambda}^{\text{floor}(j)} \leftarrow (\lambda_1, \dots, \lfloor \lambda_j \rfloor, \dots, \lambda_d)$ for all $j \in \mathcal{J}^{\text{cts}}$
  $\boldsymbol{\lambda}^{\text{ceil}(j)} \leftarrow (\lambda_1, \dots, \lceil \lambda_j \rceil, \dots, \lambda_d)$ for all $j \in \mathcal{J}^{\text{cts}}$
  $v^{\text{floor}} \leftarrow \min_{j \in \mathcal{J}} V(\boldsymbol{\lambda}^{\text{floor}(j)})$
  $v^{\text{ceil}} \leftarrow \min_{j \in \mathcal{J}} V(\boldsymbol{\lambda}^{\text{ceil}(j)})$
  if $v^{\text{floor}} \leq v^{\text{ceil}}$ **then**
    $k \leftarrow \text{argmin}_{j \in \mathcal{J}} V(\boldsymbol{\lambda}^{\text{floor}(j)})$
    $\lambda_k \leftarrow \lfloor \lambda_k \rfloor$
  else
    $k \leftarrow \text{argmin}_{j \in \mathcal{J}} V(\boldsymbol{\lambda}^{\text{ceil}(j)})$
    $\lambda_k \leftarrow \lceil \lambda_k \rceil$
  end if
  $\mathcal{J} \leftarrow \mathcal{J} \setminus \{k\}$
end while

Output: $\boldsymbol{\lambda} \in \mathcal{L}$, integer feasible solution

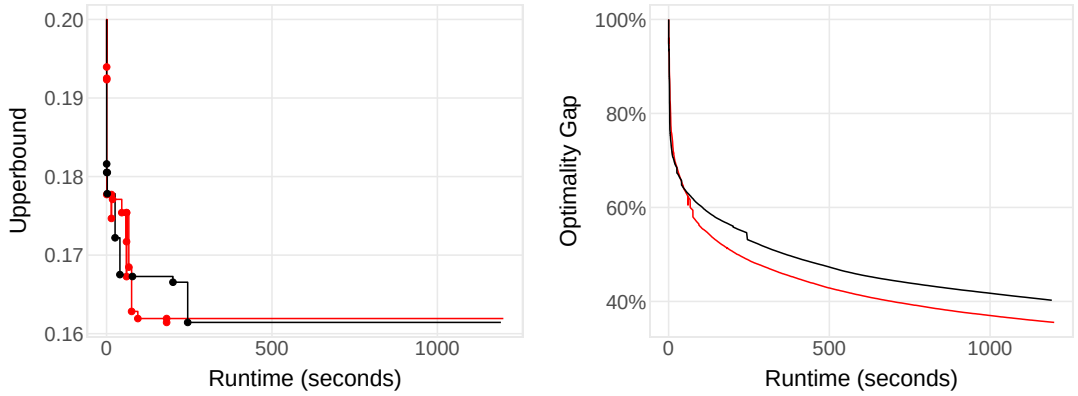

Figure 8: Performance of LCPA without rounding or polishing (black), with sequential rounding then polishing (red). We run sequential rounding in Step 14 for continuous solutions to RiskSlimLP, and the integer feasible solution using DCD. We plot large points to show when LCPA updates the incumbent solution. Results reflect performance on RiskSlimMINLP for a simulated dataset with $d = 30$ and $N = 50$'000 (see Appendix C).

4.2 Reducing the Optimality Gap

We now present two techniques to reduce the optimality gap produced by LCPA. These techniques require running LCPA with *augmented* formulations of RiskSlimMIP and RiskSlimLP shown in (6) and (7), respective (see Appendix B for IP formulations). The augmented formulations include auxiliary variables and constraints to bound the values of the objective function, loss function, and ℓ_0-norm at the optimal solution $\boldsymbol{\lambda}^*$. We aim to run LCPA with augmented formulations where these bounds are strong as possible (but still valid). In doing so, we can restrict the search region without discarding the optimal solution, thereby improves the lower bound.

AugmentedRiskSlimMIP $\left(\mathcal{L}, \mathcal{H}(\theta, \boldsymbol{\lambda}), V^{\min}, V^{\max}, L^{\min}, L^{\max}, R^{\min}, R^{\max}\right)$

$$
\begin{aligned}
\min_{\boldsymbol{\lambda}} \quad & V \\
\text{s.t.} \quad & \boldsymbol{\lambda} \in \mathcal{L} \\
& V = \theta + C_0 R \\
& \theta \in \mathcal{H}(\theta, \boldsymbol{\lambda}) \\
& R = \|\boldsymbol{\lambda}\|_0 \\
& V \in [V^{\min}, V^{\max}] \\
& \theta \in [L^{\min}, L^{\max}] \\
& R \in \{R^{\min}, \ldots, R^{\max}\}
\end{aligned}
\tag{6}
$$

$$\text{AugmentedRiskSlimLP}\left(\mathcal{L}, \mathcal{H}(\theta, \boldsymbol{\lambda}), \mathcal{P}, V^{\min}, V^{\max}, L^{\min}, L^{\max}, R^{\min}, R^{\max}\right)$$

$$\begin{aligned}
\min_{\boldsymbol{\lambda}} \quad & V \\
\text{s.t.} \quad & \boldsymbol{\lambda} \in \mathcal{P} \\
& V = \theta + C_0 R \\
& \theta \in \mathcal{H}(\theta, \boldsymbol{\lambda}) \\
& R = \sum_{j=1}^{d} \alpha_j \\
& \alpha_j = \frac{\max(\lambda_j, 0)}{\Lambda_j^{\max}} + \frac{\min(\lambda_j, 0)}{\Lambda_j^{\min}} \text{ for } j = 1, \ldots, d \\
& V \in [V^{\min}, V^{\max}] \\
& \theta \in [L^{\min}, L^{\max}] \\
& R \in [R^{\min}, R^{\max}]
\end{aligned} \tag{7}$$

4.2.1 Chained Updates

Chained updates (Algorithm 4.2.1) is a simple procedure to strengthen the values of $V^{\min}$, $V^{\max}$, $L^{\min}$, $L^{\max}$, $R^{\min}$ and $R^{\min}$ within LCPA. The procedure requires no assumptions, is easy to implement, and involves minimal computation.

Universal Bounds on Objective Value Terms

We initialize the procedure with bounds that can be computed using the training data $(\boldsymbol{x}_i, y_i)_{i=1}^N$ and the coefficient set $\mathcal{L}$. We start with Proposition 1, which yields upper and lower bounds on the logistic loss using only the fact that the coefficient set $\mathcal{L}$ is bounded.

Proposition 1 (Bounds on Logistic Loss over a Bounded Coefficient Set) *Let $(\boldsymbol{x}_i, y_i)_{i=1}^N$ denote a training dataset where $\boldsymbol{x}_i \in \mathcal{X} \subset \mathbb{R}^d$ and $y_i \in \mathcal{Y} = \{-1, +1\}$ for $i = 1, \ldots, N$. Consider the value of the normalized logistic loss function for a linear classifier with coefficients $\boldsymbol{\lambda} \in \mathcal{L} \subset \mathbb{R}^d$*

$$l(\boldsymbol{\lambda}) = \frac{1}{N} \sum_{i=1}^{N} \log(1 + \exp(-\langle \boldsymbol{\lambda}, y_i \boldsymbol{x}_i \rangle)).$$

If the coefficient set $\mathcal{L}$ is bounded, then $l(\boldsymbol{\lambda}) \in [L^{\min}, L^{\max}]$ for all $\boldsymbol{\lambda} \in \mathcal{L}$ where

$$\begin{aligned}
L^{\min} &= \frac{1}{N} \sum_{i:y_i=+1} \log\left(1 + \exp(-s_i^{\max})\right) + \frac{1}{N} \sum_{i:y_i=-1} \log\left(1 + \exp(-s_i^{\min})\right), \\
L^{\max} &= \frac{1}{N} \sum_{i:y_i=+1} \log\left(1 + \exp(-s_i^{\min})\right) + \frac{1}{N} \sum_{i:y_i=-1} \log\left(1 + \exp(-s_i^{\max})\right), \\
s_i^{\min} &= \min_{\boldsymbol{\lambda} \in \mathcal{L}} \langle \boldsymbol{\lambda}, \boldsymbol{x}_i \rangle \text{ for } i = 1, \ldots, N, \\
s_i^{\max} &= \max_{\boldsymbol{\lambda} \in \mathcal{L}} \langle \boldsymbol{\lambda}, \boldsymbol{x}_i \rangle \text{ for } i = 1, \ldots, N.
\end{aligned}$$

The value of $L^{\min}$ in Proposition 1 represents the best case loss in a perfectly separable setting when we assign each positive example the largest possible score $s_i^{\max}$, and each negative example the smallest possible score $s_i^{\min}$. Conversely, $L^{\max}$ represents the worst case loss when we assign each positive example the smallest score $s_i^{\min}$, and each negative example the largest score $s_i^{\max}$. Both $L^{\min}$ and $L^{\max}$ can be computed in $\mathrm{O}(N)$ flops using only the training data and the coefficient set by evaluating $s_i^{\min}$ and $s_i^{\max}$ as follows:

$$s_i^{\min} = \min_{\boldsymbol{\lambda}} \sum_{j=0}^{d} x_{ij}\lambda_j = \sum_{j=0}^{d} \min_{\lambda_j} x_{ij}\boldsymbol{\lambda}_j = \sum_{j=0}^{d} \mathbb{1}\left[x_{ij} > 0\right] x_{ij}\Lambda_j^{\min} + \mathbb{1}\left[x_{ij} < 0\right] x_{ij}\Lambda_j^{\max}, \quad (8)$$

$$s_i^{\max} = \max_{\boldsymbol{\lambda}} \sum_{j=0}^{d} x_{ij}\lambda_j = \sum_{j=0}^{d} \max_{\boldsymbol{\lambda}_j} x_{ij} = \sum_{j=0}^{d} \mathbb{1}\left[x_{ij} > 0\right] x_{ij}\Lambda_j^{\max} + \mathbb{1}\left[x_{ij} < 0\right] x_{ij}\Lambda_j^{\min}. \quad (9)$$

In practice, the $L^{\min}$ bound can be useful, whereas the $L^{\max}$ bound is too loose and likely to be discarded. For instance, if we have $\mathbf{0} \in \mathcal{L}$, then $l(\mathbf{0})$ yields a much tighter upper bound than $L^{\max}$. Note that $L^{\min}$ and $L^{\max}$ can also be strengthened in the following cases:

- If we have a non-trivial limit on the number of features (i.e., $R^{\max} < d$). In this case, the values of $L^{\min}$ and $L^{\max}$ are limited since $s_i^{\min}$ and $s_i^{\max}$ are also bounded by the number of non-zero coefficients. Here, $s_i^{\min}/s_i^{\max}$ can still be computed efficiently in $\mathrm{O}(N)$ flops by choosing the $R^{\max}$ smallest/largest terms in the left hand side of equation (8)/(9).
- If the training data contains multiple examples with the same features and conflicting labels. In this case, we can tighten the values of $L^{\min}$ and $L^{\max}$ by accounting for non-separable examples as follows. We let $s^+ = \sum_{i:y_i=+1,\boldsymbol{x}_i=\boldsymbol{x}^0} s_i^{\max}$ and $s^- = \sum_{i:y_i=-1,\boldsymbol{x}_i=\boldsymbol{x}^0} s_i^{\min}$ denote the total scores of training examples such that $\boldsymbol{x}_i = \boldsymbol{x}^0$ and $y_i = +1$ or $y_i = -1$, respectively. If $\log(1+\exp(-s^+)) > \log(1+\exp(-s^-))$, then we construct $L^{\max}$ by assigning the largest score $s_i^{\max}$ to all points i with $\boldsymbol{x}_i = \boldsymbol{x}^0$, and construct $L^{\min}$ by assigning the smallest score $s_i^{\min}$ to all points i with $\boldsymbol{x}_i = \boldsymbol{x}^0$ (and vice-versa if $\log(1+\exp(-s^+)) < \log(1+\exp(-s^-))$).

We can bound the number of non-zero coefficients R to $[0, d]$, trivially. In some cases, however, these bounds are stronger due to operational constraints (e.g., if we need to fit risk scores with at most 5 features, then $R \in [0, 5]$). Having initialized $L^{\min}$, $L^{\max}$, $R^{\min}$ and $R^{\min}$, we can set the bounds on the optimal objective values as $V^{\min} = L^{\min} + C_0 R^{\min}$ and $V^{\max} = L^{\max} + C_0 R^{\max}$, respectively.

Problem-Specific Bounds on Objective Value Terms

The following propositions yield stronger bounds on objective terms using bounds that are produced by the MIP solver over the course of LCPA.

Proposition 2 (Upper Bound on Optimal Number of Non-Zero Coefficients) *Given an upper bound on the optimal objective value $V^{\max} \geq V(\boldsymbol{\lambda}^*)$, and a lower bound on the optimal loss $L^{\min} \leq l(\boldsymbol{\lambda}^*)$, we can derive an upper bound on the optimal number of non-zero coefficients $R^{\max} \geq \|\boldsymbol{\lambda}^*\|_0$ as*

$$R^{\max} = \left\lfloor \frac{V^{\max} - L^{\min}}{C_0} \right\rfloor$$

Proposition 3 (Upper Bound on Optimal Loss)
Given an upper bound on the optimal objective value $V^{\max} \geq V(\boldsymbol{\lambda}^*)$*, and a lower bound on the optimal number of non-zero coefficients* $R^{\min} \leq \|\boldsymbol{\lambda}^*\|_0$*, we can derive an upper bound on the optimal loss* $L^{\max} \geq l(\boldsymbol{\lambda}^*)$ *as*

$$L^{\max} = V^{\max} - C_0 R^{\min}.$$

Proposition 4 (Lower Bound on Optimal Loss)
Given a lower bound on the optimal objective value $V^{\min} \leq V(\boldsymbol{\lambda}^*)$*, and an upper bound on the optimal number of non-zero coefficients* $R^{\max} \geq \|\boldsymbol{\lambda}^*\|_0$*, we can derive a lower bound on value of the loss function* $L^{\min} \leq l(\boldsymbol{\lambda}^*)$ *as*

$$L^{\min} = V^{\min} - C_0 R^{\max}.$$

Chained Updates Procedure

We use Propositions 2 – 4 in a simple procedure (Algorithm 5) to update the bounds in the augmented formulations of the surrogate problems, RiskSlimMIP and RiskSlimLP.

Algorithm 5 Chained Updates for LCPA

Input

C_0	ℓ_0 penalty parameter for RiskSlimMINLP
$V^{\min}$, $V^{\max}$, $L^{\min}$, $L^{\max}$, $R^{\min}$, $R^{\max}$	initial bounds on $V(\boldsymbol{\lambda}^*)$, $l(\boldsymbol{\lambda}^*)$ and $\|\boldsymbol{\lambda}^*\|_0$

1: **repeat**
2: $V^{\min} \leftarrow \max\left(V^{\min},\ L^{\min} + C_0 R^{\min}\right)$ ▷ update lower bound on $V(\boldsymbol{\lambda}^*)$
3: $V^{\max} \leftarrow \min\left(V^{\max},\ L^{\max} + C_0 R^{\max}\right)$ ▷ update upper bound on $V(\boldsymbol{\lambda}^*)$
4: $L^{\min} \leftarrow \max\left(L^{\min},\ V^{\min} - C_0 R^{\max}\right)$ ▷ update lower bound on $l(\boldsymbol{\lambda}^*)$
5: $L^{\max} \leftarrow \min\left(L^{\max},\ V^{\max} - C_0 R^{\min}\right)$ ▷ update upper bound on $l(\boldsymbol{\lambda}^*)$
6: $R^{\max} \leftarrow \min\left(R^{\max},\ \left\lfloor \frac{V^{\max} - L^{\min}}{C_0} \right\rfloor\right)$ ▷ update upper bound on $\|\boldsymbol{\lambda}^*\|_0$
7: **until** Steps 2 to 6 do not update any bounds

Output: $V^{\min}$, $V^{\max}$, $L^{\min}$, $L^{\max}$, $R^{\min}$, $R^{\max}$

Propositions 2 to 4 impose dependencies between the values of $V^{\min}$, $V^{\max}$, $L^{\min}$, $L^{\max}$, $R^{\min}$ and $R^{\max}$ that may lead to a complex "chain" of updates. As shown in Figure 4.2.1, it may be possible to update more than one of these values, and update some values more than once. Consider a case where we call the procedure once our MIP solver improves the lower bound on the objective value $V^{\min}$. If we update $L^{\min}$ on Step 4, but do not update $R^{\max}$ on Step 6, then it will not update $V^{\max}$, $L^{\min}$, $L^{\max}$, $V^{\min}$ at the next iteration. However, if $R^{\max}$ is updated after rounding, then $V^{\max}$, $L^{\min}$, $L^{\max}$, $V^{\min}$ will be updated.

In light of these dependencies, Algorithm 5 cycles through Propositions 2 to 4 until it cannot update any of the values of $V^{\min}$, $V^{\max}$, $L^{\min}$, $L^{\max}$, $R^{\min}$ and $R^{\max}$. This ensures that Algorithm 5 returns the strongest possible bounds, regardless of the value that updated in the first place. In addition, it allows us to use Algorithm 5 in settings other than LCPA such as our initialization procedure in Section 4.2.2.

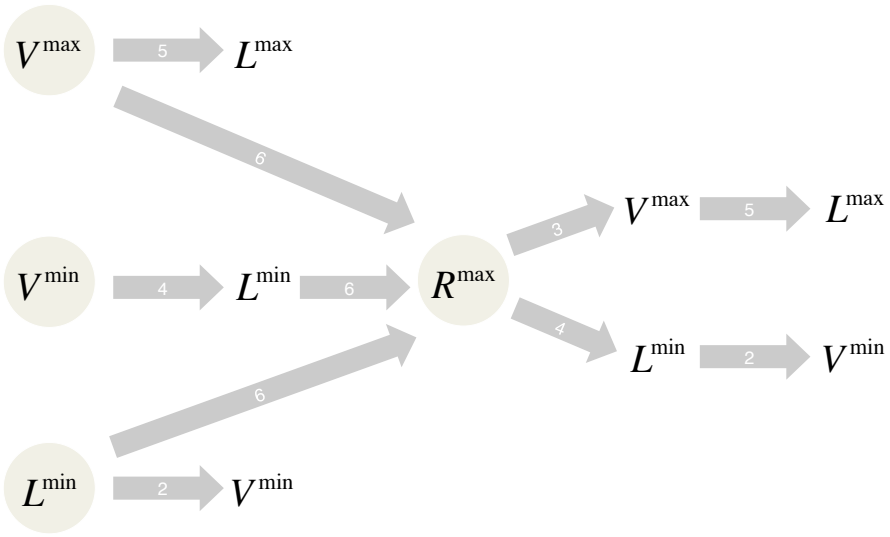

Figure 9: All possible update "chains" in Algorithm 5. We circle terms that can be updated externally by the MIP solver in LCPA. When any of these terms are updated, we run Algorithm 5 and potentially strengthen all terms in outward path marked by the arrows. The numbers inside each arrow refer to the relevant step in Algorithm 5.

In Figure 4.2.1, we show how chained updates procedure can improve the lower bound and optimality gap returned by LCPA. Here, we call Algorithm 5 whenever LCPA updates V^{max} in Step 10, or V^{min} in Step 18. If the bounds on the objective value terms improve as a result of this call, we pass this information to the MIP solver by updating the bounds in the augmented formulation shown in Appendix B.

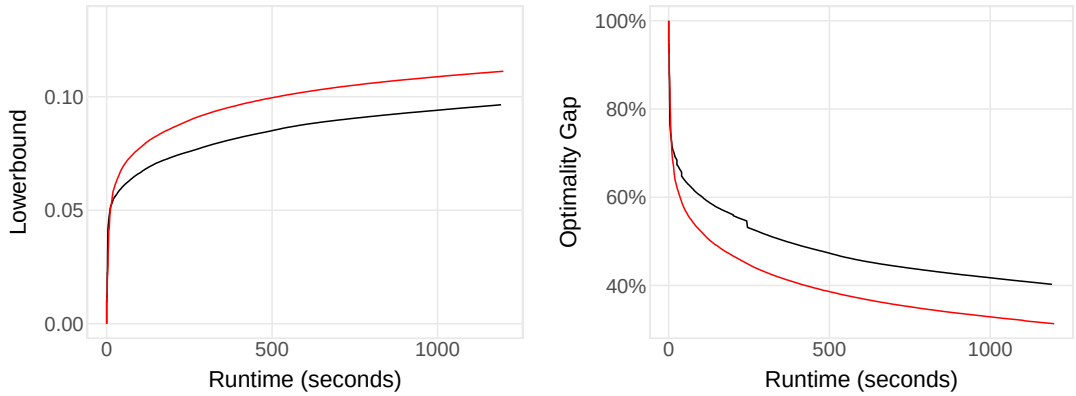

Figure 10: Performance of LCPA without chained updates (black) and with chained updates (red; Algorithm 5). Results reflect performance on an RiskSlimMINLP instance for a simulated dataset with $d = 30$ and $N = 50'000$ (see Appendix C).

4.2.2 Initialization Procedure

In Algorithm 6, we present an initialization procedure to kick-start LCPA with a high quality feasible solution, a set of initial cutting planes, and strong bounds on the optimal values of the objective function, loss function, and number of non-zero coefficients. The procedure makes use of all techniques presented so far, as follows:

1. Run CPA on RiskSlimLP: We apply CPA solve RiskSlimLP $\left(\text{conv}\left(\mathcal{L}\right), \mathcal{H}^0(\theta, \boldsymbol{\lambda})\right)$. We store the cuts from RiskSlimLP to initialize LCPA, and record the CPA lower bound on the objective value of RiskSlimLP as the initial lower bound on the optimal objective value $V^{\min}$.

2. Sequential Rounding and Polishing: For each solution produced by CPA, we run sequential rounding (Algorithm 4) to obtain an integer feasible solution for RiskSlimMINLP. We then polish this solution using DCD (Algorithm 3). We use the best solution to update the upper bound on the optimal objective value $V^{\max}$.

3. Chained Updates: Having obtained strong bounds on $V^{\min}$ and $V^{\max}$, we update all bounds using the chained updates procedure (Algorithm 5).

In Figure 11, we show the effect of the initialization procedure on the lower bound and the optimality gap.

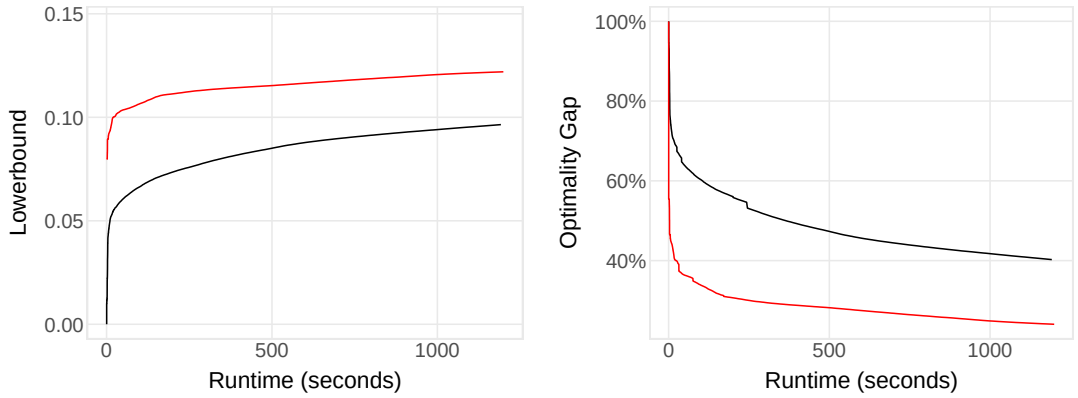

Figure 11: Performance of LCPA with no initialization (black) and with initialization (red; see Algorithm 6). Results reflect performance on an RiskSlimMINLP instance for a simulated dataset with $d = 30$ and $N = 50$'000 (see Appendix C).

Algorithm 6 Initialization Procedure for LCPA

Input

$(\boldsymbol{x}_i, y_i)_{i=1}^N$	training data
$\mathcal{L}$	constraint set for RiskSlimMINLP
C_0	ℓ_0 penalty parameter for RiskSlimMINLP
$V^{\min}$, $V^{\max}$, $L^{\min}$, $L^{\max}$, $R^{\min}$, $R^{\max}$	initial bounds on $V(\boldsymbol{\lambda}^*)$, $l(\boldsymbol{\lambda}^*)$ and $\|\boldsymbol{\lambda}^*\|_0$
$T^{\max}$	time limit for CPA on RiskSlimLP

Initialize

$\mathcal{H}^0(\theta, \boldsymbol{\lambda}) \leftarrow \{\theta \geq 0\}$ collection of cuts to the loss function

Step I: Solve RiskSlimLP using CPA

Solve RiskSlimLP $\left(\mathcal{H}^0(\theta, \boldsymbol{\lambda}), \text{conv}\left(\mathcal{L}\right)\right)$ using CPA ▷ Algorithm 1
$k \leftarrow$ number of CPA iterations completed
$\mathcal{H}^{\text{initial}}(\theta, \boldsymbol{\lambda}) \leftarrow \mathcal{H}^k(\theta, \boldsymbol{\lambda})$ ▷ store cuts to loss function from iterations 1 to k of CPA
$\mathcal{Q}^{\text{cts}} \leftarrow \{\boldsymbol{\lambda}^t\}_{t=1}^k$ ▷ store solutions to RiskSlimLP from iterations 1 to k of CPA
$V^{\min} \leftarrow$ lower bound from CPA ▷ CPA lower bound for RiskSlimLP is lower bound for $V(\boldsymbol{\lambda}^*)$

Step II: Round and Polish Continuous Solutions from CPA

for each $\boldsymbol{\lambda}^{\text{cts}} \in \mathcal{Q}^{\text{cts}}$ **do**
  $\boldsymbol{\lambda}^{\text{sr}} \leftarrow \mathsf{SequentialRounding}\left(\boldsymbol{\lambda}^{\text{cts}}, \mathcal{L}, C_0\right)$ ▷ Algorithm 4
  $\boldsymbol{\lambda}^{\text{dcd}} \leftarrow \mathsf{DiscreteCoordinateDescent}\left(\boldsymbol{\lambda}^{\text{sr}}, \mathcal{L}, C_0\right)$ ▷ Algorithm 3
  $\mathcal{Q}^{\text{int}} \leftarrow \mathcal{Q}^{\text{int}} \cup \{\boldsymbol{\lambda}^{\text{dcd}}\}$ ▷ store polished integer feasible solutions
end for
$\boldsymbol{\lambda}^{\text{best}} \leftarrow \text{argmin}_{\boldsymbol{\lambda} \in \mathcal{P}} V(\boldsymbol{\lambda})$
$V^{\max} \leftarrow V\left(\boldsymbol{\lambda}^{\text{best}}\right)$ ▷ best integer feasible solution is upper bound for $V(\boldsymbol{\lambda}^*)$

Step III: Update Bounds on Objective Value Terms

$(V^{\min}, V^{\max}, L^{\min}, L^{\max}, R^{\min}, R^{\max}) \leftarrow \mathsf{ChainedUpdates}\left(V^{\min}, \ldots, R^{\max}, C_0\right)$ ▷ Algorithm 5

Output: $\boldsymbol{\lambda}^{\text{best}}$, $\mathcal{H}^{\text{initial}}(\theta, \boldsymbol{\lambda})$, $V^{\min}$, $V^{\max}$, $L^{\min}$, $L^{\max}$, $R^{\min}$, $R^{\max}$

---

5. Reducing Data-Related Computation

In this section, we present two techniques that reduce data-related computation for the risk score problem. The reduction is achieved by exploiting the fact that coefficients belong to a bounded discrete set $\mathcal{L}$. The resulting speed up allows us to fit high quality models in less time, and for a larger range of datasets.

5.1 Fast Loss Evaluation via Lookup Tables

The first technique is designed to reduce computation when evaluating the loss function and its derivative, which can reduce the time that LCPA uses to compute cut parameters (3) and run the procedures in Section 4.1. The technique requires that the features $\boldsymbol{x}_i$ and coefficients $\boldsymbol{\lambda}$ belong to sets that are bounded, discrete, and regularly spaced, such as $\boldsymbol{x}_i \in \mathcal{X} \subseteq \{0,1\}^d$ and $\boldsymbol{\lambda} \in \mathcal{L} \subseteq \{-10,\ldots,10\}^{d+1}$.

Evaluating the logistic loss $\log(1+\exp(-\langle \boldsymbol{\lambda}, y_i \boldsymbol{x}_i \rangle))$ for a given value of $\boldsymbol{\lambda}$ is a relatively expensive computation because it involves exponentiation, and because it must be implemented in multiple steps to avoid numerical overflow/underflow when the scores $s_i := \langle \boldsymbol{\lambda}, \boldsymbol{x}_i y_i \rangle$ are too small or too large[5],

Since the training data $\mathcal{D} = (\boldsymbol{x}_i, y_i)_{i=1}^N$ and coefficients $\boldsymbol{\lambda} \in \mathcal{L}$ belong to discrete and bounded sets, the scores $s_i = \langle \boldsymbol{\lambda}, \boldsymbol{x}_i y_i \rangle$ also belong to a discrete and bounded set

$$\mathcal{S} = \left\{ \langle \boldsymbol{\lambda}, \boldsymbol{x}_i y_i \rangle \;\middle|\; i = 1,\ldots,N \text{ and } \boldsymbol{\lambda} \in \mathcal{L} \right\}.$$

If the elements of the feature set $\mathcal{X}$ and the coefficient set $\mathcal{L}$ are regularly spaced (e.g., with spacing 1), then the scores will belong to the set of integers $\mathcal{S} \subseteq \mathbb{Z} \cap [s^{\min}, s^{\max}]$ where:

$$s^{\min} = \min_{i,\boldsymbol{\lambda}} \{ \langle \boldsymbol{\lambda}, \boldsymbol{x}_i y_i \rangle \text{ for all } (\boldsymbol{x}_i, y_i) \in \mathcal{D} \text{ and } \boldsymbol{\lambda} \in \mathcal{L} \}$$
$$s^{\max} = \max_{i,\boldsymbol{\lambda}} \{ \langle \boldsymbol{\lambda}, \boldsymbol{x}_i y_i \rangle \text{ for all } (\boldsymbol{x}_i, y_i) \in \mathcal{D} \text{ and } \boldsymbol{\lambda} \in \mathcal{L} \}$$

Thus, we can precompute and store all possible values of the loss function in a lookup table with $s^{\max} - s^{\min} + 1$ rows, where row m contains the value of $[\log(1+\exp(-(m+s^{\min}-1)))]$.

This strategy can reduces the time to evaluate the loss function as we replace a computationally expensive operation with a simple lookup operation. In practice, the lookup table is usually small enough to be cached in memory, which yields a substantial runtime speedup. Further, since the values of $s^{\min}$ and $s^{\max}$ can be computed exactly in $\mathrm{O}(N)$ time, the lookup table can be narrowed down as $R^{\max}$ is updated over the course of LCPA.

As shown in Figure 5.1, the lookup table reduces the total amount of data-related computation compared to a standard high performance numerical computation library. The reduction in data-related computation may translate into a significant difference in the ability of the algorithm to return a high quality risk score, with a stronger proof of optimality under a time constraint.

5. The value of $\exp(s)$ can be computed reliably using IEEE 754 double precision floating point numbers for $s \in [-700, 700]$. The term will overflow to ∞ when $s < -700$, and underflow to 0 when when $s > 700$.

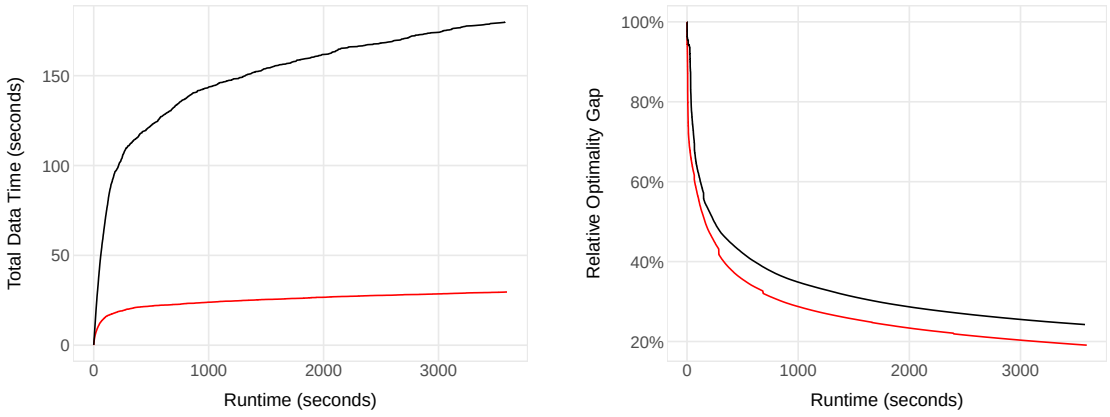

Figure 12: Time spent on data-related computation and optimality gap for LCPA when we evaluate the loss function (black) and using the lookup table (red). Results reflect performance on an RiskSlimMINLP instance for a simulated dataset with $d = 30$ and $N = 1'000'000$ (see Appendix C).

5.2 Cheaper Heuristics via Subsampling

The next technique is aims to reduce data-related computation for heuristic procedures such as sequential rounding by using a subsample of the full training dataset.

In theory, we wish to run heuristic procedures frequently as they can yield feasible solutions to RiskSlimMINLP. In practice, however, we limit the number of times we run these procedures because each run requires multiple evaluations of the loss function, and runs that fail to update the incumbent solution effectively slow down the progress of LCPA. If, for example, we ran sequential rounding each time we found a new set of continuous coefficients in LCPA, then we would spend too much time rounding, without necessarily finding a better solution.

The technique works as follows. Before running LCPA, we set aside a "heuristics" dataset $\mathcal{D}_M$ by sampling M points without replacement from the full training dataset $\mathcal{D}_N$. Once we run LCPA, we then reduce data-related computation by running all heuristics using $\mathcal{D}_M$. To distinguish between situations where the loss and objective are computed with $\mathcal{D}_M$ or $\mathcal{D}_N$, let $l_i(\boldsymbol{\lambda}) = \log(1 + \exp(\langle \boldsymbol{\lambda}, y_i \boldsymbol{x}_i, \rangle))$ and define:

$$l_M(\boldsymbol{\lambda}) = \frac{1}{M} \sum_{i=1}^{M} l_i(\boldsymbol{\lambda}), \qquad V_M(\boldsymbol{\lambda}) = l_M(\boldsymbol{\lambda}) + C_0 \left\|\boldsymbol{\lambda}\right\|_0$$

$$l_N(\boldsymbol{\lambda}) = \frac{1}{N} \sum_{i=1}^{N} l_i(\boldsymbol{\lambda}), \qquad V_N(\boldsymbol{\lambda}) = l_N(\boldsymbol{\lambda}) + C_0 \left\|\boldsymbol{\lambda}\right\|_0 .$$

Consider a case where a heuristic procedure returns a "promising" solution $\boldsymbol{\lambda}^H$ such that:

$$V_M(\boldsymbol{\lambda}^H) < V^{\max}. \tag{10}$$

In this case, we compute the objective value on the full training dataset $\mathcal{D}_N$ by evaluating the loss at each of the $N - M$ points that were not included in $\mathcal{D}_M$. As usual, we then

update the incumbent solution if $\boldsymbol{\lambda}^H$ attains an objective value that is less than the current upper bound on RiskSlimMINLP:

$$V_N(\boldsymbol{\lambda}^H) < V^{\max} \tag{11}$$

Note that although we always evaluate the loss for the full training dataset $\mathcal{D}_N$ to confirm an incumbent update, this technique still reduces data-related computation as heuristic procedures typically require us to evaluate the loss multiple times (e.g., sequential rounding requires $\frac{1}{3}d(d^2-1)$ evaluations of the loss). In the interest of reducing computation, this technique also ignores "false negative" solutions $\boldsymbol{\lambda}^H$ that do poorly on the heuristics dataset $V_M(\boldsymbol{\lambda}^H) \geq V^{\max}$ but would update the incumbent on the true dataset $V_N(\boldsymbol{\lambda}^H) < V^{\max}$.

The main draw of using the subsampling technique is the following generalization bound that guarantees that any solution that updates the incumbent when the objective is evaluated with $\mathcal{D}_M$ will also update incumbent when the objective is evaluated with $\mathcal{D}_N$ (i.e., that any solution that satisfies (10) will also satisfy (11)).

Theorem 2 (Generalization of Sampled Loss on Finite Coefficient Set) *Let $\mathcal{D}_N = (\boldsymbol{x}_i, y_i)_{i=1}^N$ denote a training dataset with $N > 1$ points, and let $\mathcal{D}_M = (\boldsymbol{x}_i, y_i)_{i=1}^M$ denote a sample of M points drawn without replacement from $\mathcal{D}_N$. Let $\boldsymbol{\lambda}$ denote the coefficients of a linear classifier from a finite set $\mathcal{L}$. For all $\varepsilon > 0$, it holds that*

$$\Pr\left(\max_{\boldsymbol{\lambda}\in\mathcal{L}}\left(l_N(\boldsymbol{\lambda}) - l_M(\boldsymbol{\lambda})\right) \geq \varepsilon\right) \leq |\mathcal{L}| \exp\left(-\frac{2\varepsilon^2}{(\frac{1}{M})(1-\frac{M}{N})(1+\frac{M}{N})\Delta^{\max}(\mathcal{L},\mathcal{D}_N)^2}\right)$$

where

$$\Delta^{\max}(\mathcal{L},\mathcal{D}_N) = \max_{\boldsymbol{\lambda}\in\mathcal{L}} \left(\max_{i=1,\ldots,N} l_i(\boldsymbol{\lambda}) - \min_{i=1,\ldots,N} l_i(\boldsymbol{\lambda})\right)$$

Theorem 2 is a generalization bound that is derived from a concentration inequality for problems where we are sampling without replacement, known as the Hoeffding-Serfling inequality (see Bardenet et al., 2015). The Hoeffding-Serfling inequality can be significantly tighter than the classical Hoeffding inequality as it ensures that $\Pr\left(l_N(\boldsymbol{\lambda}) - l_M(\boldsymbol{\lambda}) \geq \epsilon\right) \to 0$ as $M \to N$ for all $\epsilon > 0$. Here, $\Delta^{\max}(\mathcal{L},\mathcal{D}_N)$ is a normalization term that represents the maximum range of loss values on the full training dataset $\mathcal{D}_N$ for the coefficient set $\mathcal{L}$. This term can be computed cheaply using the smallest and largest values of the coefficients and features as shown in Proposition 1 (Section 4.2.1).

In general, the $|\mathcal{L}|$ term in Theorem 2 produces a bound that is too loose to be useful. In the case of rounding heuristics, however, it effectively limits the difference between $l_N(\boldsymbol{\lambda})$ and $l_M(\boldsymbol{\lambda})$ since the feasible coefficient set $\mathcal{L}$ contains at most 2^d possible values. In this setting, Theorem 2 can be used to assess the probability that a proposed incumbent update will lead to an actual incumbent update, as shown in Corollary 1. Alternatively, it can be used to choose the size of the subsampled dataset M so as to guarantee that an incumbent update on $\mathcal{D}_M$ will yield an incumbent update on $\mathcal{D}_N$. In either case, the bound can be strengthened by recomputing the normalization term $\Delta^{\max}(\mathcal{L}(\boldsymbol{\rho}),\mathcal{D}_N)$ separately for each continuous solution ρ, or periodically over the course of LCPA (as the MIP solver reduces the set of feasible coefficients via branch-and-bound).

Corollary 1 (Update Probabilities of Rounding Heuristics on Sampled Data) *Consider a rounding heuristic that takes as input a vector of continuous coefficients* $\boldsymbol{\rho} = (\rho_1, \ldots, \rho_d) \in \text{conv}(\mathcal{L})$ *and produces as output a vector of integer coefficients* $\boldsymbol{\lambda} \in \mathcal{L}(\boldsymbol{\rho})$ *where*

$$\mathcal{L}(\boldsymbol{\rho}) = \left(\boldsymbol{\lambda} \in \mathcal{L} \;\middle|\; \lambda_j \in \{\lceil \rho_j \rceil, \lfloor \rho_j \rfloor\} \text{ for } j = 1, \ldots, d\right)$$

Consider evaluating the rounding heuristic using a sample of M *points* $\mathcal{D}_M = (\boldsymbol{x}_i, y_i)_{i=1}^M$ *drawn without replacement from the full training dataset* $\mathcal{D}_N = (\boldsymbol{x}_i, y_i)_{i=1}^N$. *Pick a tolerance* $\delta > 0$. *Given rounded coefficients* $\boldsymbol{\lambda} \in \mathcal{L}(\boldsymbol{\rho})$, *compute* $V_M(\boldsymbol{\lambda})$. *If*

$$V_M(\boldsymbol{\lambda}) < V^{\max} - \varepsilon_\delta,$$

then w.p. at least $1 - \delta$, *we have*

$$V_N(\boldsymbol{\lambda}) \leq V^{\max}$$

where

$$\varepsilon_\delta = \Delta^{\max}(\mathcal{L}(\boldsymbol{\rho}), \mathcal{D}_N) \sqrt{\frac{\log(1/\delta) + d\log(2)}{2} \left(1 - \frac{M}{N}\right) \left(1 + \frac{M}{N}\right)}.$$

6. Benchmarking

In this section, we benchmark data-driven methods to learn risk scores with few terms and small integer coefficients. In addition to our proposed method, we consider baseline methods that process the coefficients of penalized logistic regression models using the rounding and polishing techniques from Section 4.1, or techniques that are used in practice.

6.1 Setup

Datasets: We ran experiments on 6 publicly available datasets shown in Table 2. We picked these datasets to explore the performance of each method as we varied the size and nature of the training data. Other than `arrest`, all datasets can be found at the UCI ML repository (Lichman, 2013). The `arrest` dataset must be requested from ICPSR as described in Zeng et al. (2015). We processed each dataset by binarizing all categorical features and some real-valued features. For the purposes of reproducibility, we include all processed datasets other than `arrest` with our final submission.

Dataset	Source	Classification Task
`adult`	Kohavi (1996)	predict if a U.S. resident earns more than $50 000
`arrest`	Zeng et al. (2015)	predict if a prisoner will be arrested within 3 years of release
`bank`	Moro et al. (2014)	predict if person signs up for bank account after marketing call
`mammo`	Elter et al. (2007)	detect breast cancer using a mammogram
`mushroom`	Schlimmer (1987)	predict if a mushroom is poisonous
`spambase`	Cranor and LaMacchia (1998)	predict if an e-mail is spam

Table 2: Datasets used for benchmarking experiments.

Methods: For each dataset, we fit a risk score with small integer coefficients $\lambda_j \in [-5, 5]$ and limited model size $\|\boldsymbol{\lambda}\|_0 \leq 5$ to match risk scores that are currently used in practice (see e.g., Gage et al., 2001). We used a total of 8 methods, described below.

- RiskSLIM (Optimized Risk Score): We formulate an instance of RiskSlimMINLP with the following constraints: $\lambda_0 \in \{-100, \ldots, 100\}$, $\lambda_j \in \{-5, \ldots, 5\}$, and $\|\boldsymbol{\lambda}\|_0 \leq 5$. We set the trade-off parameter to a small value ($C_0 = 10^{-8}$) so that the optimizer belongs to the C_0–level set of feasible models (if C_0 is small enough, then this corresponds to the best-fitting model that satisfies all constraints). We solve each instance using LCPA along with the improvements in Sections 4 and 5. We cap total runtime for each instance at 20 minutes, and solve it using the CPLEX 12.6.3 Python API on a 3.33GHz CPU with 16GB RAM.

- PLR (Penalized Logistic Regression): We fit logistic regression models with a combined $\ell_1 + \ell_2$ penalty using the glmnet package in R 3.2.3 (Friedman et al., 2010). We consider models for 1100 free parameter instances: 11 values of the elastic-net mixing parameter $alpha \in \{0.0, 0.1, \ldots, 1.0\} \times 100$ values of the regularization penalty $lambda$ picked by glmnet. We include explicit constraints to bound $\lambda_j \in [-5, 5]$ for $j = 1, \ldots, d$.

- Rd (PLR + Naive Rounding): We fit a pool of models using PLR. For each model in the pool, we round each coefficient to the nearest integer in $\{-5, \ldots, 5\}^d$ by setting

$\lambda_j \leftarrow \lceil \min(\max(\lambda_j, -5), 5) \rfloor$ for $j = 1, \ldots, d$, and round the intercept to the nearest integer by setting $\lambda_0 \leftarrow \lceil \lambda_0 \rfloor$.

- RsRd (PLR + Rescaled Rounding): We fit a pool of models using PLR. For each model in the pool, we rescale all coefficients so that the largest coefficient is 5 or -5, and then round them to the nearest integer (i.e., $\lambda_j \rightarrow \lceil \gamma \lambda_j \rfloor$ where $\gamma = 5/\max_{j=1,\ldots,d}(|\lambda_j|)$). Here, rescaling is meant to prevent rounding λ_j to zero when $\lambda_j \in [-0.5, 0.5]$.

- SeqRd (PLR + Sequential Rounding): We fit a pool of models using PLR. For each model in the pool, we round the coefficients using sequential rounding (Algorithm 4).

- Rd*/RsRd*/SeqRd* (Polished Versions of Rd/RsRd/SeqRd): We fit a pool of models using Rd/RsRd/SeqRd and polish the coefficients using DCD (Algorithm 3). To ensure that the number of non-zero coefficients does not increase (which would violate the model size constraint), we only run DCD on the set of non-zero coefficients $\{j \mid \lambda_j \neq 0\}$.

Performance Metrics: We evaluated all models in terms of the following metrics.

- Rank Accuracy: We used the standard area under the ROC curve (AUC).

- Sparsity: We used a metric known as *model size*, which represents the number of non-zero coefficients and does not count the coefficient for the intercept.

- Risk Calibration: We constructed *reliability diagrams* which plot, for each distinct score, the predicted risk on the x-axis against the observed risk on the y-axis[6] (see DeGroot and Fienberg, 1983). We summarize calibration across the entire reliability diagram using the *calibration error* (CAL), which represents the root mean squared error between the predicted risk and the observed risk[7] (see Caruana and Niculescu-Mizil, 2004, 2006). A model with perfect calibration yields predicted risk estimates that are perfectly aligned with observed values, meaning that the points on the reliability diagram should fall on the $x = y$ line, and CAL should equal 0.0%.

Model Selection and Assessment: We used standard nested 5-fold cross-validation (5-CV) to select a final model and assess its predictive accuracy. We fit a final model using all of training data using the instance of the free parameters that: (i) satisfied the model size constraint; and (ii) maximized the 5-CV mean test AUC. Since 5-CV statistics are used to select the final model, they provide an optimistic measure of expected performance for the final model. To avoid this bias, we use a nested CV setup where we ran the aforementioned model selection procedure for each fold. Explicitly, for each of the 5 "outer" folds, we ran an "inner" 5-CV and fit a final model using all the data for that fold. We picked a final model for each outer fold using the free parameter instances that: (i) satisfied the model size constraint; and (ii) maximized the inner 5-CV mean test AUC.

6. We estimate the observed risk for each distinct score s as $p(s) = \frac{1}{N(s)} \sum_{i:s=s_i} \mathbb{1}[y_i = +1]$ where s_i is the score for example i. For clarity, when a risk score has over 30 distinct scores (i.e., when the data contains real-valued features or the model uses real-valued coefficients), we construct the reliability diagram by binning scores into 10 equally spaced bins from 0 to 1.
7. CAL is defined as $\frac{1}{N}\sqrt{\sum_s \sum_{i:s_i=s}(p_i - p(s))^2}$ where s_i and p_i is the predicted score and risk for example i, and $N(s)$ is the number of observations with a score of s.

6.2 Results

In Table 3, we summarize the performance of risk scores from all methods on all datasets. In Figure 13, we include reliability diagrams to show the risk calibration of the risk scores from Table 3 in greater detail. In Figures 14 and 15, we plot ℓ_0-regularization paths to show how the AUC and CAL of risk scores change with the model size constraint. In Figures 16 to 18, we show risk scores for `arrest`, `adult` and `bank` built using RiskSLIM. In what follows, we briefly discuss these results.

On Performance

As shown in Table 2, RiskSLIM models have superior risk calibration and rank accuracy compared to models built with other methods. Specifically, RiskSLIM models have the best 5-CV mean test AUC (i.e., *test AUC*) on 5/6 datasets, and the best 5-CV mean test CAL (i.e., *test CAL*) on 6/6 datasets. In comparison, models built using the baseline methods (i.e., all methods other than PLR) perform slightly worse in terms of test AUC and can significantly worse in terms of test CAL. As shown in Figures 14 and 15, the relative performance advantages of RiskSLIM models are more notable for smaller model sizes – which is beneficial since most risk scores that are currently deployed have few terms.

Most of these results can be explained by noting that: (i) models with good risk calibration typically attain low values of the logistic loss (as shown in Table 3, and observed by Caruana and Niculescu-Mizil, 2004); and, (ii) since we are fitting from a simple class of models, almost all risk scores in Table 2 generalize well (i.e., the test AUC/CAL is very close to their training AUC/CAL). In particular, RiskSLIM models attain the lowest value of the logistic loss since they are fit by minimizing the loss over exact constraints on model form. Accordingly, the models perform well in terms of training CAL as per (i), and (subsequently) in terms of test CAL as per (ii). In the same way, baseline methods such as Rd*, RsRd* and SeqRd* can fit models that attain lower values of the loss because they use loss minimizing heuristics, such as DCD polishing or sequential rounding. As such, the resulting models have improved risk calibration compared to models from methods that do not use these techniques (i.e, RsRd, Rd, and SeqRd).

The results in Table 2 suggest a similar relationship between the logistic loss and rank accuracy, but this has some caveats. In particular, a method such as RsRd, can provably improve AUC by rescaling coefficients before rounding. However, given that the logistic loss is not scale invariant, the rescaled models attain high values of the logistic loss and poor risk calibration (see e.g., the reliability diagrams for RsRd in Figure 13). In addition, it is possible for a model that attains the minimum logistic loss but not have the best training AUC (see e.g., `mammo` where the RiskSLIM model has an optimality gap of 0.0%).

On Computation

RiskSLIM is the only method to pair models with a measure of optimality. Although the risk score problem is $\mathcal{NP}$-hard, we fit models with small optimality gaps in 20 minutes by pairing LCPA with the techniques in Sections 4 and 5.

Our experience also highlighted some practical benefits that are difficult to measure. In particular, RiskSLIM could build and evaluate risk scores without the need for nested cross-validation. This important given that the baseline methods required us to run the

rounding and polishing techniques and then compute the AUC for all 33'000 models that we fit (vs. 6 for RiskSLIM). Thus, the resulting training process could take far longer than the time used to fit RiskSLIM, especially on large datasets.

On Pitfalls and Best-Practices for Heuristic Approaches

Our results show that the performance of risk scores built with heuristic approaches may vary depending on a range of issues, including: the techniques used for rounding; the constraints on model form; the range of features in the dataset. In some cases, risk scores built by just rounding coefficients to the nearest integer perform well (see e.g, RD on `bank`). In others, however, performance can falter (see e.g., RD for `spambase`). In practice, it may be difficult to identify performance issues without thoroughly evaluating both rank accuracy *and* risk calibration since: (i) popular techniques may produce models that with good AUC but poor CAL (e.g., RsRd, used by Pennsylvania Commission on Sentencing, 2012); and (ii) summary statistics such as AUC and CAL may not provide a clear picture of performance over the entire ROC curve and reliability diagram. The fact that risk scores built with heuristic approaches may have inconsistent or suboptimal performance highlights the importance of the optimality gap, as this can help users tell if risk scores perform due to restrictive constraints or approximations in the technique. The optimality gap is especially valuable in this setting, since PLR models, which are used as a baseline for risk scores, may also perform poorly due to suboptimal feature selection or overfitting (see e.g., Table 3).

Our results broadly suggest the following best practices for heuristic approaches.

1. Use a loss-minimizing rounding or polishing procedure, ideally SeqRd*

2. Run model selection after rounding since this preserves a large pool of models from which to choose. If we were to run any model selection procedure on the pool of PLR models, and then round the coefficients from that model, then we could dramatically alter the value of the loss, and thereby performance.

3. Use a model selection produce that optimizes the K-CV AUC instead of the K-CV CAL. In fitting models, we compared both techniques. As expected, we found that switching the model selection procedure that optimizes the mean 5-CV test CAL produces models that perform slightly better in terms of CAL (though not good as RiskSLIM), however, could have far worse AUC. This is because the CAL metric weights calibration based on the number of people at each predicted probability, so trivial models may sometimes have low CAL on problems with class imbalance.

4. Binarize real-valued features. On datasets that contain real-valued features at different scales (e.g,, `spambase`), PLR may assign small coefficients to important features that have large values. In such cases, rounding techniques set any coefficient $\lambda_j \in [-0.5, 0.5]$ to 0, removing them the model and impacting performance. This issue is surprisingly difficult to address without binarizing features. Normalizing features can greatly affect usability since it means that users would also have to normalize features when making predictions with the resulting risk score or avoid using small integer coefficients. An alternative solution is to rescale the coefficients before rounding (RsRd), but this can affect risk calibration given that the logistic loss is not scale invariant (see e.g., the reliability diagrams for RsRd in Figure 13).

Dataset	Details	Metric	PLR	RD	RSRD	SEQRD	RD*	RSRD*	SEQRD*	RISKSLIM
adult	$N = 32561$ $d = 36$	**test auc**	0.817	0.830	0.830	0.830	0.832	0.832	0.832	0.854
		test cal	5.5%	4.3%	9.1%	4.3%	4.2%	6.3%	4.2%	2.6%
		model size	4	4	4	4	4	4	4	5
		loss value	0.451	0.417	0.484	0.417	0.417	0.458	0.417	0.385
		optimality gap	-	-	-	-	-	-	-	9.7%
arrest	$N = 22530$ $d = 48$	**test auc**	0.700	0.691	0.691	0.691	0.677	0.690	0.677	0.697
		test cal	7.5%	5.7%	20.8%	5.7%	3.8%	15.6%	3.8%	1.7%
		model size	5	5	5	5	4	5	4	5
		loss value	0.638	0.626	1.282	0.626	0.624	0.895	0.624	0.609
		optimality gap	-	-	-	-	-	-	-	4.0%
bank	$N = 41188$ $d = 57$	**test auc**	0.725	0.759	0.759	0.759	0.760	0.749	0.760	0.760
		test cal	2.2%	1.4%	9.5%	1.4%	1.3%	7.2%	1.3%	1.3%
		model size	2	5	5	5	5	2	5	5
		loss value	0.339	0.289	0.953	0.289	0.289	0.333	0.289	0.289
		optimality gap	-	-	-	-	-	-	-	3.5%
mammo	$N = 961$ $d = 14$	**test auc**	0.845	0.845	0.845	0.845	0.845	0.836	0.845	0.843
		test cal	7.3%	8.1%	15.3%	8.1%	7.4%	7.2%	7.4%	5.0%
		model size	3	3	3	3	3	3	3	5
		loss value	0.482	0.480	0.624	0.480	0.480	0.496	0.480	0.469
		optimality gap	-	-	-	-	-	-	-	0.0%
mushroom	$N = 8124$ $d = 113$	**test auc**	0.976	0.973	0.977	0.973	0.978	0.980	0.978	0.989
		test cal	20.9%	12.3%	6.5%	12.3%	5.4%	3.1%	5.4%	1.8%
		model size	5	5	5	5	5	5	5	5
		loss value	0.362	0.200	0.162	0.200	0.144	0.139	0.144	0.069
		optimality gap	-	-	-	-	-	-	-	18.0%
spambase	$N = 4601$ $d = 57$	**test auc**	0.823	0.908	0.862	0.908	0.908	0.913	0.908	0.928
		test cal	10.5%	24.2%	23.6%	24.2%	17.9%	10.3%	17.9%	11.7%
		model size	4	5	5	5	5	5	5	5
		loss value	0.553	0.472	5.670	0.472	0.402	0.381	0.402	0.349
		optimality gap	-	-	-	-	-	-	-	33.4%

Table 3: Performance of risk scores with model size $\|\boldsymbol{\lambda}\|_0 \leq 5$ and integer coefficients $\lambda_j \in \{-5, \ldots, 5\}$. Note PLR models have real-valued coefficients $\lambda_j \in [-5, 5]$. Here: *test auc* is the 5-CV mean test AUC; *test cal* is the 5-CV mean test calibration error; *model size* is the model size of the final model; *loss value* is the value of the logistic loss for the final model; *optimality gap* is the relative optimality gap of the final model.

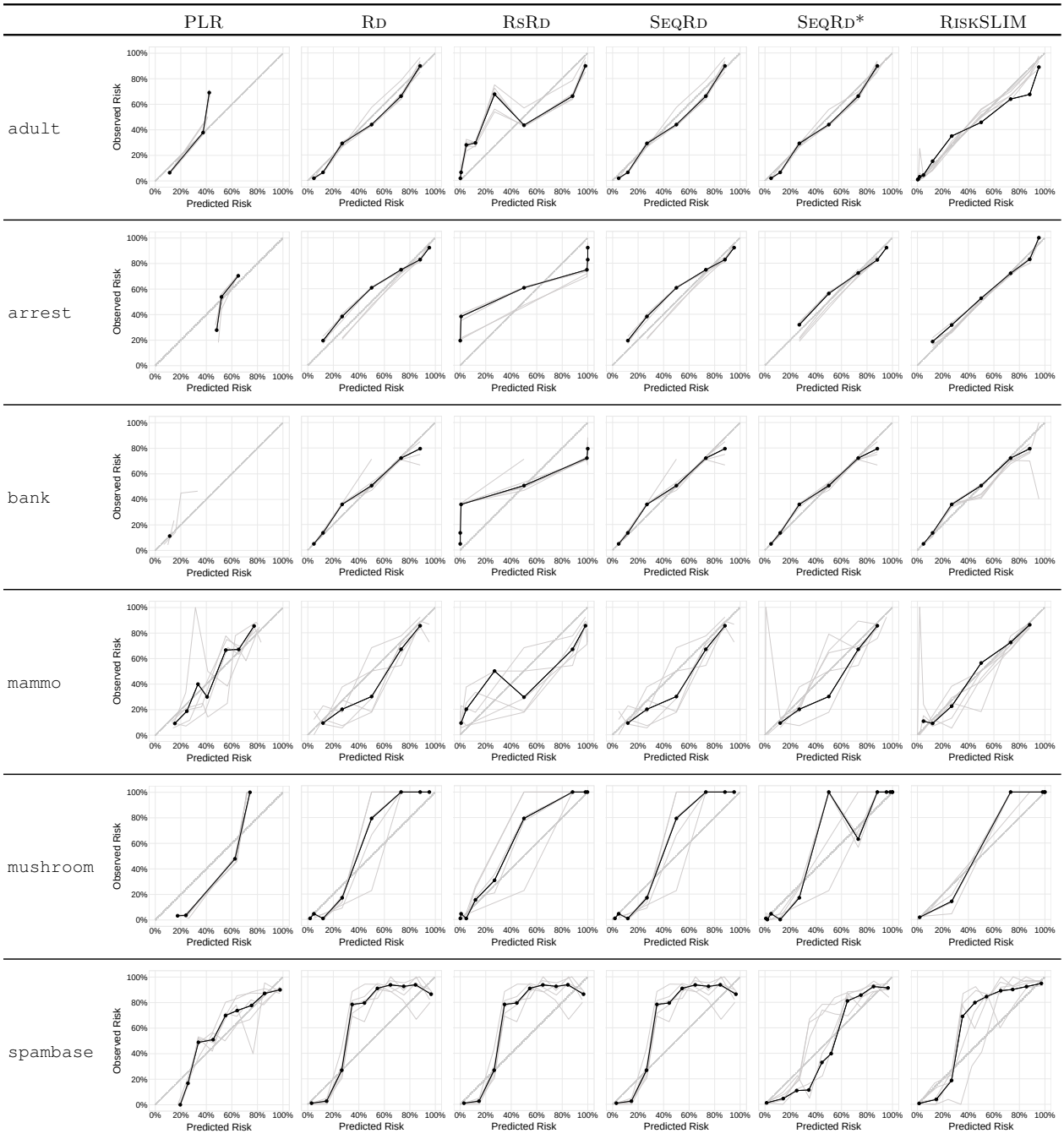

Figure 13: Reliability diagrams for risk scores with model size $\|\boldsymbol{\lambda}\|_0 \leq 5$ and integer coefficients $\lambda_j \in \{-5, \ldots, 5\}$. We include results for PLR as a baseline since they have real-valued coefficients $\lambda_j \in [-5, 5]$. We plot results for fold models on test data in grey, and for the final model on training data in black.

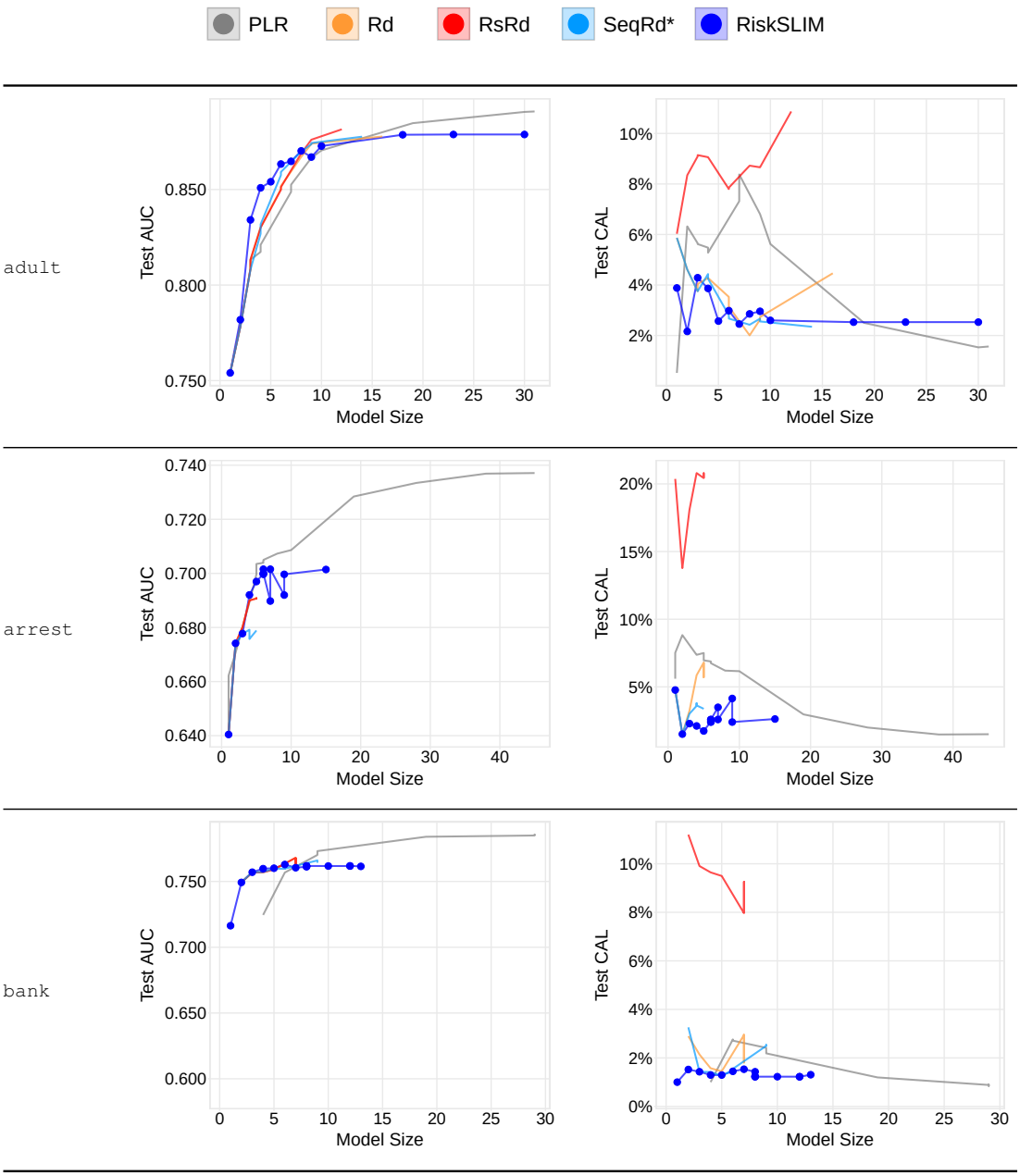

Figure 14: Test AUC (left) and Test CAL (right) of risk scores with integer coefficients $\lambda_j \in \{-5, \ldots, 5\}$ and model sizes $\|\boldsymbol{\lambda}\|_0 \leq R^{\max}$ for $R^{\max} \in \{1, 2, \ldots, 10, 20, 30, 40, 50, \infty\}$. Note PLR risk scores have real-valued coefficients $\lambda_j \in [-5, 5]$.

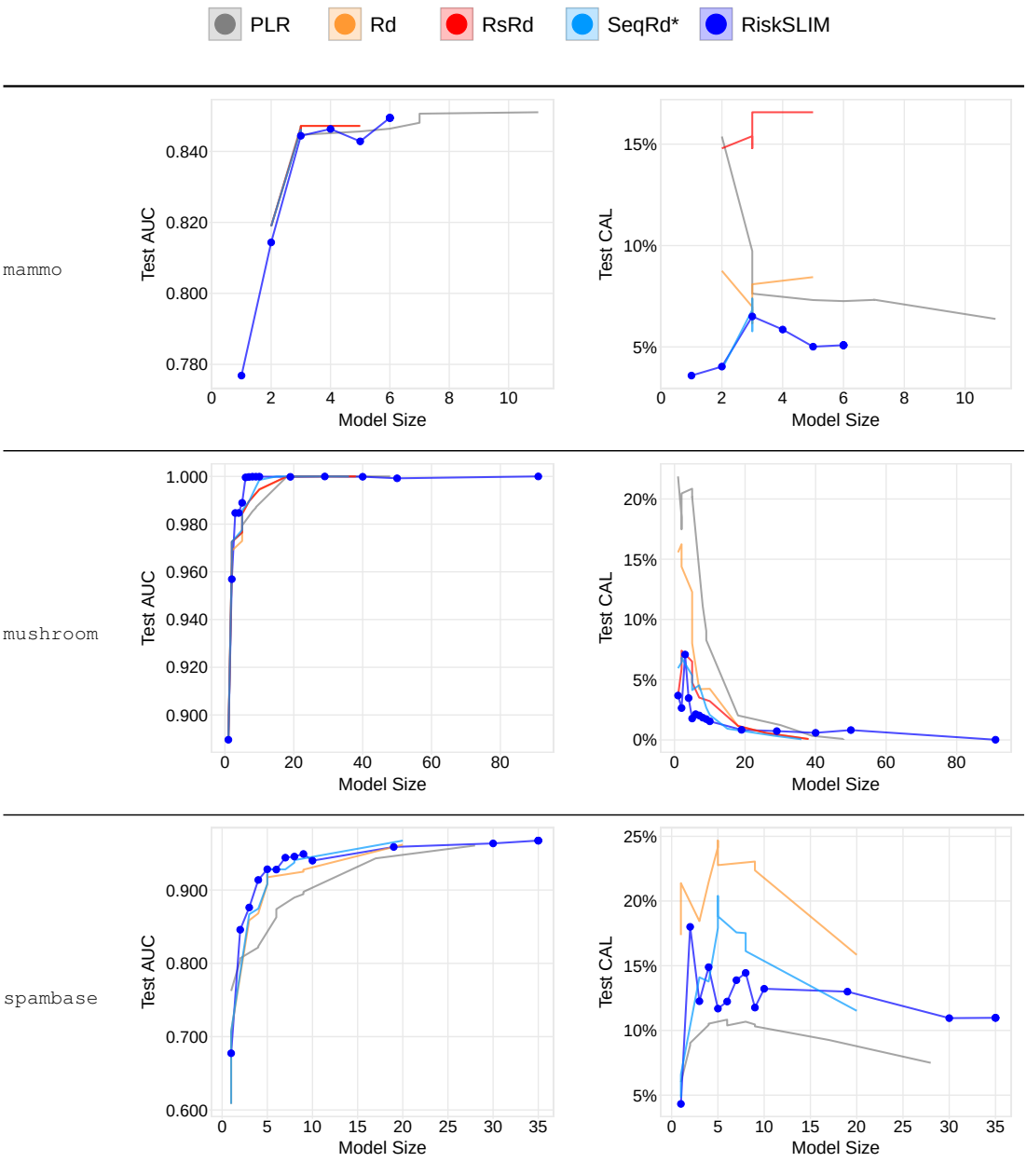

Figure 15: Test AUC (left) and Test CAL (right) of risk scores with integer coefficients $\lambda_j \in \{-5, \ldots, 5\}$ and model sizes $\|\boldsymbol{\lambda}\|_0 \leq R^{\max}$ for $R^{\max} \in \{1, 2, \ldots, 10, 20, 30, 40, 50, \infty\}$. Note PLR risk scores have real-valued coefficients $\lambda_j \in [-5, 5]$.

1.	*Prior Arrests* ≥ 2	1 point		$\cdots\cdots$
2.	*Prior Arrests* ≥ 5	1 point	$+$	$\cdots\cdots$
3.	*Prior Arrests for Local Ordinance*	1 point	$+$	$\cdots\cdots$
4.	*Age at Release between* 18 *to* 24	1 point	$+$	$\cdots\cdots$
5.	*Age at Release* ≥ 40	-1 points	$+$	$\cdots\cdots$
	ADD POINTS FROM ROWS 1–5	**SCORE**	$=$	$\cdots\cdots$

SCORE	-1	0	1	2	3	4
RISK	11.9%	26.9%	50.0%	73.1%	88.1%	95.3%

Figure 16: RiskSLIM model for `arrest`. RISK represents the predicted probability that a prisoner is arrested for any offense within 3 years of release from prison. This model has a 5-CV mean test AUC/CAL of 0.697/1.7% and training AUC/CAL of 0.701/2.6%.

1.	*Married*	3 points		$\cdots\cdots$
2.	*Reported Capital Gains*	2 points	$+$	$\cdots\cdots$
3.	*Age between* 22 *to* 29	-1 point	$+$	$\cdots\cdots$
4.	*Highest Level of Education is High School Diploma*	-2 points	$+$	$\cdots\cdots$
5.	*No High School Diploma*	-3 points	$+$	$\cdots\cdots$
	ADD POINTS FROM ROWS 1 –5	**SCORE**	$=$	$\cdots\cdots$

SCORE	≤ -1	0	1	2	3	4	5
RISK	5.0%	11.9	26.9%	50.0%	73.1%	88.1%	95.3

Figure 17: RiskSLIM model for `adult`. RISK represents the predicted probability that a US resident earns over \$50 000. This model has a 5-CV mean test AUC/CAL of 0.854/2.4% and training AUC/CAL of 0.860/4.1%.

1.	*Call between January and March*	1 point		$\cdots\cdots$
2.	*Called Previously*	1 point	$+$	$\cdots\cdots$
3.	*Previous Call was Successful*	1 point	$+$	$\cdots\cdots$
4.	*Employment Indicator* < 5100	1 point	$+$	$\cdots\cdots$
5.	3 *Month Euribor Rate* ≥ 100	-1 point	$+$	$\cdots\cdots$
	ADD POINTS FROM ROWS 1 –5	**SCORE**	$=$	$\cdots\cdots$

SCORE	-1	0	1	2	3	4
RISK	4.7%	11.9	26.9%	50.0%	73.1%	88.1%

Figure 18: RiskSLIM model for `bank`. RISK represents the predicted probability that a client opens a new bank account after a marketing call. This model has a 5-CV mean test AUC/CAL of 0.760/1.3% and a training AUC/CAL of 0.760/1.1%.

7. Discussion

Our goal in this paper was to develop a principled new approach to build risk scores, which are models that are extensively used in high-stakes applications but currently built using ad hoc methods. To this end, we first formulated a difficult optimization problem to fit a risk score that is fully optimized for feature selection, small integer coefficients, and operational constraints. We then solved this problem by developing a cutting plane method that does not stall on non-convex problems, and pairing this method with techniques to generate feasible solutions, narrow the optimality gap, and reduce data-related computation.

An important characteristic of our proposed improvements is that they are more powerful when used together. For instance, using sequential rounding and polishing to generate a feasible solution can lead to a tighter bound on the number of features through chained updates, which can then lead to faster computation by reducing the size of the lookup table.

As shown through our results, the optimal solution to our problem leads to significant performance benefits in terms of AUC and risk-calibration – especially when fitting from heavily constrained model classes that are typical for risk scores. Aside from performance benefits, our approach had several practical benefits, namely: (i) it can fit models that obey complex operational constraints without parameter tuning, which greatly reduces the number of models that need to be fit to build and evaluate a risk score; (ii) it can assess the optimality of each model, which can help users tell if poor performance is due to the model class or the fitting process.

Acknowledgments

We gratefully acknowledge support from Siemens and Wistron. We would like to thank Paul Rubin for countless helpful discussions.

References

Amaldi, Edoardo and Viggo Kann. On the approximability of minimizing nonzero variables or unsatisfied relations in linear systems. *Theoretical Computer Science*, 209(1):237–260, 1998.

Atkinson, David S and Pravin M Vaidya. A cutting plane algorithm for convex programming that uses analytic centers. *Mathematical Programming*, 69(1-3):1–43, 1995.

Austin, James, Roger Ocker, and Avi Bhati. Kentucky pretrial risk assessment instrument validation. *Bureau of Justice Statistics. Grant*, (2009-DB), 2010.

Bai, Lihui and Paul A Rubin. Combinatorial Benders Cuts for the Minimum Tollbooth Problem. *Operations Research*, 57(6):1510–1522, 2009. doi: 10.1287/opre.1090.0694. URL http://or.journal.informs.org/cgi/content/abstract/opre.1090.0694v1.

Bardenet, Rémi, Odalric-Ambrym Maillard, and others. Concentration inequalities for sampling without replacement. *Bernoulli*, 21(3):1361–1385, 2015.

Bobko, Philip, Philip L Roth, and Maury A Buster. The usefulness of unit weights in creating composite scores. A literature review, application to content validity, and meta-analysis. *Organizational Research Methods*, 10(4):689–709, 2007.

Bonami, Pierre, Mustafa Kilinç, and Jeff Linderoth. Algorithms and software for convex mixed integer nonlinear programs. In *Mixed integer nonlinear programming*, pages 1–39. Springer, 2012.

Boyd, Stephen P and Lieven Vandenberghe. *Convex optimization*. Cambridge university press, 2004.

Burgess, Ernest W. Factors determining success or failure on parole. *The workings of the indeterminate sentence law and the parole system in Illinois*, pages 221–234, 1928.

Bussieck, Michael R and Stefan Vigerske. Minlp solver software. *Wiley Encyclopedia of Operations Research and Management Science*, 2010.

Byrd, Richard H, Jorge Nocedal, and Richard A Waltz. Knitro: An integrated package for nonlinear optimization. In *Large-scale nonlinear optimization*, pages 35–59. Springer, 2006.

Carrizosa, Emilio, Amaya Nogales-Gómez, and Dolores Romero Morales. Strongly agree or strongly disagree?: Rating features in support vector machines. *Information Sciences*, 329:256–273, 2016.

Caruana, Rich and Alexandru Niculescu-Mizil. Data mining in metric space: an empirical analysis of supervised learning performance criteria. In *Proceedings of the tenth ACM SIGKDD international conference on Knowledge discovery and data mining*, pages 69–78. ACM, 2004.

Caruana, Rich and Alexandru Niculescu-Mizil. An empirical comparison of supervised learning algorithms. In *Proceedings of the 23rd international conference on Machine learning*, pages 161–168. ACM, 2006.

Chevaleyre, Yann, Frédéerick Koriche, and Jean-Daniel Zucker. Rounding methods for discrete linear classification. In *Proceedings of the 30th International Conference on Machine Learning (ICML-13)*, pages 651–659, 2013.

Cowan, Nelson. The magical mystery four how is working memory capacity limited, and why? *Current directions in psychological science*, 19(1):51–57, 2010.

Cranor, Lorrie Faith and Brian A LaMacchia. Spam! *Communications of the ACM*, 41(8):74–83, 1998.

DeGroot, Morris H and Stephen E Fienberg. The comparison and evaluation of forecasters. *The statistician*, pages 12–22, 1983.

Duwe, Grant and KiDeuk Kim. Sacrificing accuracy for transparency in recidivism risk assessment: The impact of classification method on predictive performance. *Corrections*, pages 1–22, 2016.

Dwork, Cynthia, Moritz Hardt, Toniann Pitassi, Omer Reingold, and Richard Zemel. Fairness through awareness. In *Proceedings of the 3rd Innovations in Theoretical Computer Science Conference*, pages 214–226. ACM, 2012.

Efron, Bradley, Trevor Hastie, Iain Johnstone, and Robert Tibshirani. Least angle regression. *The Annals of Statistics*, 32(2):407–499, 2004.

Elter, M, R Schulz-Wendtland, and T Wittenberg. The prediction of breast cancer biopsy outcomes using two cad approaches that both emphasize an intelligible decision process. *Medical Physics*, 34:4164, 2007.

Ertekin, Şeyda and Cynthia Rudin. A bayesian approach to learning scoring systems. *Big Data*, 3 (4):267–276, 2015.

Franc, Vojtěch and Soeren Sonnenburg. Optimized cutting plane algorithm for support vector machines. In *Proceedings of the 25th international conference on Machine learning*, pages 320–327. ACM, 2008.

Franc, Vojtěch and Sören Sonnenburg. Optimized cutting plane algorithm for large-scale risk minimization. *The Journal of Machine Learning Research*, 10:2157–2192, 2009.

Friedman, Jerome, Trevor Hastie, and Robert Tibshirani. Regularization paths for generalized linear models via coordinate descent. *Journal of Statistical Software*, 33(1):1–22, 2010.

Gage, Brian F, Amy D Waterman, William Shannon, Michael Boechler, Michael W Rich, and Martha J Radford. Validation of clinical classification schemes for predicting stroke. *The Journal of the American Medical Association*, 285(22):2864–2870, 2001.

Gary, Michael R and David S Johnson. Computers and intractability: A guide to the theory of np-completeness, 1979.

Goel, Sharad, Justin M Rao, and Ravi Shroff. Precinct or prejudice? understanding racial disparities in new york city's stop-and-frisk policy. *Understanding Racial Disparities in New York City's Stop-and-Frisk Policy (March 2, 2015)*, 2015.

Goffin, Jean-Louis and Jean-Philippe Vial. Convex nondifferentiable optimization: A survey focused on the analytic center cutting plane method. *Optimization Methods and Software*, 17(5):805–867, 2002.

Goodman, Bryce and Seth Flaxman. Eu regulations on algorithmic decision-making and a" right to explanation". *arXiv preprint arXiv:1606.08813*, 2016.

Hübner, Ruth and Anita Schöbel. When is rounding allowed in integer nonlinear optimization? *European Journal of Operational Research*, 237(2):404–410, 2014.

Jennings, D, TM Amabile, and L Ross. Informal covariation assessment: Data-based vs. theory-based judgments. *Judgment under uncertainty: Heuristics and biases*, pages 211–230, 1982.

Joachims, Thorsten. Training linear svms in linear time. In *Proceedings of the 12th ACM SIGKDD international conference on Knowledge discovery and data mining*, pages 217–226. ACM, 2006.

Joachims, Thorsten, Thomas Finley, and Chun-Nam John Yu. Cutting-plane training of structural svms. *Machine Learning*, 77(1):27–59, 2009.

Kamishima, Toshihiro, Shotaro Akaho, and Jun Sakuma. Fairness-aware learning through regularization approach. In *2011 IEEE 11th International Conference on Data Mining Workshops*, pages 643–650. IEEE, 2011.

Kelley, James E, Jr. The cutting-plane method for solving convex programs. *Journal of the Society for Industrial and Applied Mathematics*, 8(4):703–712, 1960.

Knaus, William A, Jack E Zimmerman, Douglas P Wagner, Elizabeth A Draper, and Diane E Lawrence. APACHE-acute physiology and chronic health evaluation: a physiologically based classification system. *Critical Care Medicine*, 9(8):591–597, 1981.

Knaus, William A, Elizabeth A Draper, Douglas P Wagner, and Jack E Zimmerman. APACHE II: a severity of disease classification system. *Critical Care Medicine*, 13(10):818–829, 1985.

Knaus, William A, DP Wagner, EA Draper, JE Zimmerman, Marilyn Bergner, PG Bastos, CA Sirio, DJ Murphy, T Lotring, and A Damiano. The APACHE III prognostic system. risk prediction of hospital mortality for critically ill hospitalized adults. *Chest Journal*, 100(6):1619–1636, 1991.

Kodratoff, Y. The comprehensibility manifesto. *KDD Nugget Newsletter*, 94(9), 1994.

Kohavi, Ron. Scaling up the accuracy of naive-bayes classifiers: A decision-tree hybrid. In *KDD*, pages 202–207, 1996.

Kotlowski, Wojciech, Krzysztof J Dembczynski, and Eyke Huellermeier. Bipartite ranking through minimization of univariate loss. In *Proceedings of the 28th International Conference on Machine Learning (ICML-11)*, pages 1113–1120, 2011.

Latessa, Edward, Paula Smith, Richard Lemke, Matthew Makarios, and Christopher Lowenkamp. Creation and validation of the ohio risk assessment system: Final report. *Center for Criminal Justice Research, School of Criminal Justice, University of Cincinnati, Cincinnati, OH. Retrieved from http://www. ocjs. ohio. gov/ORAS_FinalReport. pd f*, 2009.

Le Gall, Jean-Roger, Philippe Loirat, Annick Alperovitch, Paul Glaser, Claude Granthil, Daniel Mathieu, Philippe Mercier, Remi Thomas, and Daniel Villers. A simplified acute physiology score for icu patients. *Critical Care Medicine*, 12(11):975–977, 1984.

Le Gall, Jean-Roger, Stanley Lemeshow, and Fabienne Saulnier. A new simplified acute physiology score (SAPS II) based on a european/north american multicenter study. *The Journal of the American Medical Association*, 270(24):2957–2963, 1993.

Letham, Benjamin, Cynthia Rudin, Tyler H McCormick, and David Madigan. An interpretable stroke prediction model using rules and bayesian analysis. 2013.

Levin, A Yu. On an algorithm for the minimization of convex functions. In *Soviet Mathematics Doklady*, volume 160, pages 1244–1247, 1965.

Lichman, M. UCI machine learning repository, 2013. URL http://archive.ics.uci.edu/ml.

Malioutov, Dmitry M and Kush R Varshney. Exact rule learning via boolean compressed sensing. In *ICML (3)*, pages 765–773, 2013.

Mangasarian, Olvi L, W Nick Street, and William H Wolberg. Breast cancer diagnosis and prognosis via linear programming. *Operations Research*, 43(4):570–577, 1995.

Menon, Aditya Krishna, Xiaoqian J Jiang, Shankar Vembu, Charles Elkan, and Lucila Ohno-Machado. Predicting accurate probabilities with a ranking loss. In *Machine learning: proceedings of the International Conference. International Conference on Machine Learning*, volume 2012, page 703. NIH Public Access, 2012.

Miller, Alan J. Selection of subsets of regression variables. *Journal of the Royal Statistical Society. Series A (General)*, pages 389–425, 1984.

Moreno, Rui P, Philipp GH Metnitz, Eduardo Almeida, Barbara Jordan, Peter Bauer, Ricardo Abizanda Campos, Gaetano Iapichino, David Edbrooke, Maurizia Capuzzo, and Jean-Roger Le Gall. SAPS 3 - from evaluation of the patient to evaluation of the intensive care unit. part 2: Development of a prognostic model for hospital mortality at icu admission. *Intensive Care Medicine*, 31(10):1345–1355, 2005.

Moro, Sérgio, Paulo Cortez, and Paulo Rita. A data-driven approach to predict the success of bank telemarketing. *Decision Support Systems*, 62:22–31, 2014.

Naoum-Sawaya, Joe and Samir Elhedhli. An interior-point Benders based branch-and-cut algorithm for mixed integer programs. *Annals of Operations Research*, 210(1):33–55, November 2010.

Nguyen, Tan and Scott Sanner. Algorithms for direct 0-1 loss optimization in binary classification. In *ICML (3)*, pages 1085–1093, 2013.

Park, Jaehyun and Stephen Boyd. Concave quadratic cuts for mixed-integer quadratic problems. *arXiv preprint arXiv:1510.06421*, 2015a.

Park, Jaehyun and Stephen Boyd. A semidefinite programming method for integer convex quadratic minimization. *arXiv preprint arXiv:1504.07672*, 2015b.

Pennsylvania Commission on Sentencing, . Interim Report 4: Development of Risk Assessment Scale. Technical report, June 2012.

Reid, Mark D and Robert C Williamson. Composite binary losses. *The Journal of Machine Learning Research*, 11:2387–2422, 2010.

Ridgeway, Greg. The pitfalls of prediction. *NIJ Journal,* National Institute of Justice, 271:34–40, 2013.

Schlimmer, Jeffrey Curtis. Concept acquisition through representational adjustment. 1987.

Teo, Choon Hui, Alex Smola, SVN Vishwanathan, and Quoc Viet Le. A scalable modular convex solver for regularized risk minimization. In *Proceedings of the 13th ACM SIGKDD international conference on Knowledge discovery and data mining*, pages 727–736. ACM, 2007.

Teo, Choon Hui, S Vishwanathan, Alex Smola, and Quoc V Le. Bundle methods for regularized risk minimization. *Journal of Machine Learning Research*, 1:55, 2009.

U.S. Department of Justice, . The Mathematics of Risk Classification: Changing Data into Valid Instruments for Juvenile Courts. July 2005.

Ustun, Berk and Cynthia Rudin. Supersparse linear integer models for optimized medical scoring systems. *Machine Learning*, pages 1–43, 2015. ISSN 0885-6125. doi: 10.1007/s10994-015-5528-6. URL http://dx.doi.org/10.1007/s10994-015-5528-6.

Zafar, Muhammad Bilal, Isabel Valera, Manuel Gomez Rodriguez, and Krishna P Gummadi. Fairness constraints: A mechanism for fair classification. *arXiv preprint arXiv:1507.05259*, 2015.

Zeng, Jiaming, Berk Ustun, and Cynthia Rudin. Interpretable classification models for recidivism prediction. *arXiv preprint arXiv:1503.07810*, 2015.

Zou, Hui and Trevor Hastie. Regularization and variable selection via the elastic net. *Journal of the Royal Statistical Society: Series B (Statistical Methodology)*, 67(2):301–320, 2005.

Appendix A. Proofs

A.1 Proof of Remark 1

Remark 3 (Convergence of Lattice Cutting Plane Algorithm)
For any training dataset $(\boldsymbol{x}_i, y_i)_{i=1}^N$*, trade-off parameter* $C_0 \geq 0$*, and finite coefficient set* $\mathcal{L} \subseteq \mathbb{Z}^{d+1}$*, the lattice cutting plane algorithm (Algorithm 2) returns an optimal solution to the risk score problem* RiskSlimMINLP *after computing at most* $|\mathcal{L}|$ *cutting planes and processing at most* $2^{D(\mathcal{L})} - 1$ *nodes. Here:*

$$D(\mathcal{L}) = \prod_{j=0}^{d} (\Lambda_j^{max} - \Lambda_j^{min} + 1).$$

Proof

We will first explain why LCPA attains the optimal objective value, and then justify the upper bounds on the cutting planes and nodes.

Observe LCPA finds the optimal solution to RiskSlimMINLP through an exhaustive search over the feasible region $\mathcal{L}$. Thus, LCPA is bound to encounter the optimal solution, since it only discards a node $(V^s, \mathcal{P}^s)$ if the surrogate problem is infeasible over $\mathcal{P}^s$ (in which case RiskSlimMINLP is also infeasible over $\mathcal{P}^s$), or if the surrogate problem has an objective value that exceeds than $V^{\max}$ (in which case, there any integer feasible solution $\mathcal{P}^s$ is also suboptimal).

The bound on the number of cuts follows from the fact that Algorithm 2 only adds cuts at integer feasible solutions, of which there are at most $|\mathcal{L}|$. The bound on the number of processed nodes represents a worst-case limit produced by bounding the depth of the branch-and-bound tree. To do this, we exploit the fact that the splitting rule PartitionSplittingRule splits a partition into two mutually exclusive subsets by adding integer-valued bounds such $\lambda_j \geq \lceil \lambda_j \rceil$ and $\lambda_j \leq \lfloor \lambda_j \rfloor - 1$ on a single coefficient to the feasible solution. Consider applying PartitionSplittingRule a total of $\Lambda_j^{\max} - \Lambda_j^{\min} + 1$ times in succession on a fixed dimension j. This results in a total of $\Lambda_j^{\max} - \Lambda_j^{\min} + 1$ nodes where each node fixes the coefficient in dimension j to an integer value $\lambda_j \in \{\Lambda_j^{\min}, \ldots, \Lambda_j^{\max}\}$. Pick any node and repeat this process for coefficients in the remaining dimensions. The resulting branch and bound tree will have at most $D(\mathcal{L})$ leaf nodes where $\boldsymbol{\lambda}$ is restricted to integer feasible solutions. ■

A.2 Proof of Proposition 1

Proposition 1 (Bounds on Logistic Loss over a Bounded Coefficient Set)
Let $(\boldsymbol{x}_i, y_i)_{i=1}^N$ *denote a training dataset where* $\boldsymbol{x}_i \in \mathcal{X} \subset \mathbb{R}^d$ *and* $y_i \in \mathcal{Y} = \{-1, +1\}$ *for all* $i = 1, \ldots, N$*. Consider the value of the normalized logistic loss function for linear classifiers with coefficients* $\boldsymbol{\lambda} \in \mathcal{L} \subset \mathbb{R}^d$ *:*

$$l(\boldsymbol{\lambda}) = \frac{1}{N} \sum_{i=1}^{N} \log(1 + \exp(-\langle \boldsymbol{\lambda}, y_i \boldsymbol{x}_i \rangle))$$

If the coefficient set $\mathcal{L}$ is bounded, then $l(\boldsymbol{\lambda}) \in [L^{\min}, L^{\max}]$ for all $\boldsymbol{\lambda} \in \mathcal{L}$ where:

$$
\begin{aligned}
L^{\min} &= \frac{1}{N} \sum_{i:y_i=+1} \log\left(1+\exp(-s_i^{\max})\right) + \frac{1}{N} \sum_{i:y_i=-1} \log\left(1+\exp(-s_i^{\min})\right), \\
L^{\max} &= \frac{1}{N} \sum_{i:y_i=+1} \log\left(1+\exp(-s_i^{\min})\right) + \frac{1}{N} \sum_{i:y_i=-1} \log\left(1+\exp(-s_i^{\max})\right), \\
s_i^{\min} &= \min_{\boldsymbol{\lambda}\in\mathcal{L}} \langle \boldsymbol{\lambda}, \boldsymbol{x}_i \rangle \quad \textit{for } i = 1, \ldots, N, \\
s_i^{\max} &= \max_{\boldsymbol{\lambda}\in\mathcal{L}} \langle \boldsymbol{\lambda}, \boldsymbol{x}_i \rangle \quad \textit{for } i = 1, \ldots, N.
\end{aligned}
$$

Proof Since the coefficient set $\mathcal{L}$ is bounded, the data are $(\boldsymbol{x}_i, y_i)_{i=1}^N$ bounded, and the normalized logistic loss function $l(\boldsymbol{\lambda})$ is continuous, it follows that the value of $l(\boldsymbol{\lambda})$ is also bounded:

$$
l(\boldsymbol{\lambda}) \in [\min_{\boldsymbol{\lambda}\in\mathcal{L}} l(\boldsymbol{\lambda}), \max_{\boldsymbol{\lambda}\in\mathcal{L}}, l(\boldsymbol{\lambda})] \text{ for all } \boldsymbol{\lambda} \in \mathcal{L}.
$$

Thus we only need to show that $L^{\min} \leq \min_{\boldsymbol{\lambda}\in\mathcal{L}} l(\boldsymbol{\lambda})$, and $L^{\max} \geq \max_{\boldsymbol{\lambda}\in\mathcal{L}} l(\boldsymbol{\lambda})$. For the lower bound, we observe that:

$$
\begin{aligned}
\min_{\boldsymbol{\lambda}\in\mathcal{L}} l(\boldsymbol{\lambda}) &= \min_{\boldsymbol{\lambda}\in\mathcal{L}} \frac{1}{N} \sum_{i=1}^{N} \log(1+\exp(-\langle \boldsymbol{\lambda}, y_i \boldsymbol{x}_i \rangle)) \\
&\geq \frac{1}{N} \sum_{i=1}^{N} \min_{\boldsymbol{\lambda}\in\mathcal{L}} \ \log(1+\exp(-\langle \boldsymbol{\lambda}, y_i \boldsymbol{x}_i \rangle)) \\
&= \frac{1}{N} \sum_{i=1}^{N} \log(1+\exp(-\max_{\boldsymbol{\lambda}\in\mathcal{L}} \langle \boldsymbol{\lambda}, y_i \boldsymbol{x}_i \rangle)) \qquad (12) \\
&= \frac{1}{N} \sum_{i:y_i=+1} \log(1+\exp(-\max_{\boldsymbol{\lambda}\in\mathcal{L}} \langle \boldsymbol{\lambda}, \boldsymbol{x}_i \rangle)) + \frac{1}{N} \sum_{i:y_i=-1} \log(1+\exp(-\min_{\boldsymbol{\lambda}\in\mathcal{L}} \langle \boldsymbol{\lambda}, \boldsymbol{x}_i \rangle)) \\
&= \frac{1}{N} \sum_{i:y_i=+1} \log(1+\exp(-s_i^{\min}) + \frac{1}{N} \sum_{i:y_i=-1} \log(1+\exp(-s_i^{\max})) \\
&= L^{\min}.
\end{aligned}
$$

Here (12) follows from the fact that the logistic loss function is monotonically decreasing in $-\langle \boldsymbol{\lambda}, y_i \boldsymbol{x}_i \rangle$.

Similarly, for the upper bound, we observe that:

$$\begin{aligned}
\max_{\boldsymbol{\lambda}\in\mathcal{L}} l(\boldsymbol{\lambda}) &= \max_{\boldsymbol{\lambda}\in\mathcal{L}} \frac{1}{N}\sum_{i=1}^{N} \log(1+\exp(-\langle\boldsymbol{\lambda}, y_i\boldsymbol{x}_i\rangle)) \\
&\leq \frac{1}{N}\sum_{i=1}^{N} \max_{\boldsymbol{\lambda}\in\mathcal{L}} \log(1+\exp(-\langle\boldsymbol{\lambda}, y_i\boldsymbol{x}_i\rangle)) \\
&= \frac{1}{N}\sum_{i=1}^{N} \log(1+\exp(-\min_{\boldsymbol{\lambda}\in\mathcal{L}}\langle\boldsymbol{\lambda}, y_i\boldsymbol{x}_i\rangle)) \qquad (13)\\
&= \frac{1}{N}\sum_{i:y_i=+1} \log(1+\exp(-\min_{\boldsymbol{\lambda}\in\mathcal{L}}\langle\boldsymbol{\lambda}, \boldsymbol{x}_i\rangle)) + \frac{1}{N}\sum_{i:y_i=-1} \log(1+\exp(-\max_{\boldsymbol{\lambda}\in\mathcal{L}}\langle\boldsymbol{\lambda}, \boldsymbol{x}_i\rangle)) \\
&= \frac{1}{N}\sum_{i:y_i=+1} \log(1+\exp(-s_i^{\min}) + \frac{1}{N}\sum_{i:y_i=-1} \log(1+\exp(-s_i^{\max})) \\
&= L^{\max}.
\end{aligned}$$

■

A.3 Proof of Proposition 2

Proposition 2 (Upper Bound on Optimal Number of Non-Zero Coefficients) *Given an upper bound on the objective value $V^{\max} \geq V(\boldsymbol{\lambda}^*)$, and a lower bound on the loss function $L^{\min} \leq l(\boldsymbol{\lambda}^*)$, we can derive an upper bound on the value of the number of optimal non-zero coefficients $R^{\max} \geq \|\boldsymbol{\lambda}^*\|_0$ as*

$$R^{\max} = \left\lfloor \frac{V^{\max} - L^{\min}}{C_0} \right\rfloor$$

Proof We are given that $V^{\max} \geq V(\boldsymbol{\lambda}^*)$ where $V(\boldsymbol{\lambda}^*) := l(\boldsymbol{\lambda}^*) + C_0\|\boldsymbol{\lambda}^*\|_0$ by definition. Thus, we can recover the upper bound from Proposition 2 as follows:

$$\begin{aligned}
l(\boldsymbol{\lambda}^*) + C_0\|\boldsymbol{\lambda}^*\|_0 &\leq V^{\max}, \\
\|\boldsymbol{\lambda}^*\|_0 &\leq \frac{V^{\max} - l(\boldsymbol{\lambda}^*)}{C_0}, \\
\|\boldsymbol{\lambda}^*\|_0 &\leq \frac{V^{\max} - L^{\min}}{C_0}, \qquad (14)\\
\|\boldsymbol{\lambda}^*\|_0 &\leq \left\lfloor \frac{V^{\max} - L^{\min}}{C_0} \right\rfloor. \qquad (15)
\end{aligned}$$

Here, (14) follows from the fact that $L^{\min} \leq l(\boldsymbol{\lambda}^*)$ by definition, and (15) follows from the fact that the number of non-zero coefficients is a natural number. ■

A.4 Proof of Proposition 3

Proposition 3 (Upper Bound on Optimal Loss)
Given an upper bound on the objective value $V^{\max} \geq V(\boldsymbol{\lambda}^*)$, and a lower bound on the number of non-zero coefficients $R^{\min} \leq \|\boldsymbol{\lambda}^*\|_0$, we can derive an upper bound on value of the loss function $L^{\max} \geq l(\boldsymbol{\lambda}^*)$ where

$$L^{\max} = V^{\max} - C_0 R^{\min}.$$

Proof We are given that $V^{\max} \geq V(\boldsymbol{\lambda}^*)$ where $V(\boldsymbol{\lambda}^*) := l(\boldsymbol{\lambda}^*) + C_0 \|\boldsymbol{\lambda}^*\|_0$ by definition. Thus, we can recover the upper bound from Proposition 3 as follows:

$$\begin{aligned} l(\boldsymbol{\lambda}^*) + C_0 \|\boldsymbol{\lambda}^*\|_0 &\leq V^{\max}, \\ l(\boldsymbol{\lambda}^*) &\leq V^{\max} - C_0 \|\boldsymbol{\lambda}^*\|_0, \\ l(\boldsymbol{\lambda}^*) &\leq V^{\max} - C_0 R^{\min}. \end{aligned}$$

Here, the last line follows from the fact that $R^{\min} \leq \|\boldsymbol{\lambda}^*\|_0$ by definition. ■

A.5 Proof of Proposition 4

Proposition 4 (Lower Bound on Optimal Loss)
Given a lower bound on the objective value $V^{\min} \leq V(\boldsymbol{\lambda}^*)$, and an upper bound on the number of non-zero coefficients $R^{\max} \geq \|\boldsymbol{\lambda}^*\|_0$, we can derive a lower bound on value of the loss function $L^{\min} \leq l(\boldsymbol{\lambda}^*)$ where

$$L^{\min} = V^{\min} - C_0 R^{\min}.$$

Proof We are given that $V^{\min} \leq V(\boldsymbol{\lambda}^*)$ where $V(\boldsymbol{\lambda}^*) := l(\boldsymbol{\lambda}^*) + C_0 \|\boldsymbol{\lambda}^*\|_0$ by definition. Thus, we can recover the lower bound from Proposition 4 as follows:

$$\begin{aligned} l(\boldsymbol{\lambda}^*) + C_0 \|\boldsymbol{\lambda}^*\|_0 &\geq V^{\min}, \\ l(\boldsymbol{\lambda}^*) &\geq V^{\min} - C_0 \|\boldsymbol{\lambda}^*\|_0, \\ l(\boldsymbol{\lambda}^*) &\geq V^{\min} - C_0 R^{\max}. \end{aligned}$$

Here, the last line follows from the fact that $R^{\max} \geq \|\boldsymbol{\lambda}^*\|_0$ by definition. ■

A.6 Proof of Theorem 2

Theorem 1 (Generalization of Sampled Loss on Finite Coefficient Set) *Let $\mathcal{D}_N = (\boldsymbol{x}_i, y_i)_{i=1}^N$ denote a finite training set composed of $N > 1$ points and $\mathcal{D}_M = (\boldsymbol{x}_i, y_i)_{i=1}^M$ denote a sample of M points drawn without replacement from $\mathcal{D}_N$. Let $\boldsymbol{\lambda}$ denote the coefficients of a linear classifier from a finite set $\mathcal{L}$. Then, for all $\varepsilon > 0$, we have that*

$$\Pr\left(\max_{\boldsymbol{\lambda}\in\mathcal{L}}\left(l_N(\boldsymbol{\lambda}) - l_M(\boldsymbol{\lambda})\right) \geq \varepsilon\right) \leq |\mathcal{L}| \exp\left(-\frac{2\varepsilon^2}{(\frac{1}{M})(1-\frac{M}{N})(1+\frac{M}{N})\Delta^{\max}(\mathcal{L},\mathcal{D}_N)^2}\right)$$

where

$$\Delta^{\max}(\mathcal{L},\mathcal{D}_N) = \max_{\boldsymbol{\lambda}\in\mathcal{L}} \left(\max_{i=1,\ldots,N} l_i(\boldsymbol{\lambda}) - \min_{i=1,\ldots,N} l_i(\boldsymbol{\lambda})\right).$$

Proof For a fixed set coefficients $\boldsymbol{\lambda} \in \mathcal{L}$, consider a finite sample of N points composed of the values for the loss function $l_i(\boldsymbol{\lambda})$ for each example in the full training dataset $\mathcal{D}_N = (\boldsymbol{x}_i, y_i)_{i=1}^N$. Let $l_N(\boldsymbol{\lambda}) = \frac{1}{N}\sum_{i=1}^N l_i(\boldsymbol{\lambda})$ and $l_M(\boldsymbol{\lambda}) = \frac{1}{M}\sum_{i=1}^M l_i(\boldsymbol{\lambda})$. Then, the Hoeffding-Serfling inequality (see e.g., Theorem 2.4 in Bardenet et al., 2015) guarantees the following for all $\varepsilon > 0$:

$$\Pr\left(l_N(\boldsymbol{\lambda}) - l_M(\boldsymbol{\lambda}) \geq \varepsilon\right) \leq \exp\left(-\frac{2\varepsilon^2}{(\frac{1}{M})(1-\frac{M}{N})(1+\frac{M}{N})\Delta(\boldsymbol{\lambda},\mathcal{D}_N)^2}\right)$$

where

$$\Delta(\boldsymbol{\lambda},\mathcal{D}_N) = \max_{i=1,\ldots,N} l_i(\boldsymbol{\lambda}) - \min_{i=1,\ldots,N} l_i(\boldsymbol{\lambda}).$$

We recover the desired inequality by generalizing this bound to hold for all $\boldsymbol{\lambda} \in \mathcal{L}$ as follows.

$$\begin{aligned}
\Pr\left(\max_{\boldsymbol{\lambda}\in\mathcal{L}}\left(l_N(\boldsymbol{\lambda}) - l_M(\boldsymbol{\lambda})\right) \geq \varepsilon\right) &= \Pr\left(\bigcup_{\boldsymbol{\lambda}\in\mathcal{L}} \left(l_N(\boldsymbol{\lambda}) - l_M(\boldsymbol{\lambda}) \geq \varepsilon\right)\right), \\
&\leq \sum_{\boldsymbol{\lambda}\in\mathcal{L}} \Pr\left(l_N(\boldsymbol{\lambda}) - l_M(\boldsymbol{\lambda}) \geq \varepsilon\right), \qquad (16) \\
&\leq \sum_{\boldsymbol{\lambda}\in\mathcal{L}} \exp\left(-\frac{2\varepsilon^2}{(\frac{1}{M})(1-\frac{M}{N})(1+\frac{M}{N})\Delta(\boldsymbol{\lambda},\mathcal{D}_N)^2}\right), \qquad (17) \\
&\leq |\mathcal{L}| \exp\left(-\frac{2\varepsilon^2}{(\frac{1}{M})(1-\frac{M}{N})(1+\frac{M}{N})\Delta^{\max}(\mathcal{L},\mathcal{D}_N)^2}\right). \qquad (18)
\end{aligned}$$

Here, (16) follows from the union bound, (17) follows from the Hoeffding Serling inequality, (18) follows from the fact that $\Delta(\boldsymbol{\lambda},\mathcal{D}_N) \leq \Delta^{\max}(\mathcal{L},\mathcal{D}_N)$ given that $\boldsymbol{\lambda} \in \mathcal{L}$. ■

A.7 Proof of Corollary 1

Corollary 1 (Update Probabilities of Rounding Heuristics on Sampled Data) *Consider a rounding heuristic that takes as input a vector of continuous coefficients* $\boldsymbol{\rho} = (\rho_1, \ldots, \rho_d) \in \text{conv}(\mathcal{L})$ *and produces as output a vector of integer coefficients* $\boldsymbol{\lambda} \in \mathcal{L}(\boldsymbol{\rho})$ *where*

$$\mathcal{L}(\boldsymbol{\rho}) = \left(\boldsymbol{\lambda} \in \mathcal{L} \;\middle|\; \lambda_j \in \{\lceil \rho_j \rceil, \lfloor \rho_j \rfloor\} \;\; \textit{for } j = 1, \ldots, d\right)$$

Consider evaluating the rounding heuristic using a sample of M *points* $\mathcal{D}_M = (\boldsymbol{x}_i, y_i)_{i=1}^M$ *drawn without replacement from the full training dataset* $\mathcal{D}_N = (\boldsymbol{x}_i, y_i)_{i=1}^N$. *Pick a tolerance* $\delta > 0$. *Given rounded coefficients* $\boldsymbol{\lambda} \in \mathcal{L}(\boldsymbol{\rho})$, *compute* $V_M(\boldsymbol{\lambda})$. *If*

$$V_M(\boldsymbol{\lambda}) < V^{\max} - \varepsilon_\delta,$$

then w.p. at least $1 - \delta$, *we have*

$$V_N(\boldsymbol{\lambda}) \leq V^{\max}$$

Proof We will first show that for any tolerance that we pick $\delta > 0$, the prescribed choice of ε_δ will ensure that $V_N(\boldsymbol{\lambda}) - V_M(\boldsymbol{\lambda}) \leq \varepsilon_\delta$ w.p. at least $1 - \delta$. Restating the result of Theorem 2, we have that for any $\varepsilon > 0$:

$$\Pr\left(\max_{\boldsymbol{\lambda} \in \mathcal{L}} \left(l_N(\boldsymbol{\lambda}) - l_M(\boldsymbol{\lambda})\right) \geq \varepsilon\right) \leq |\mathcal{L}| \exp\left(-\frac{2\varepsilon^2}{(\frac{1}{M})(1 - \frac{M}{N})(1 + \frac{M}{N})\Delta^{\max}(\mathcal{L}, \mathcal{D}_N)^2}\right). \quad (19)$$

Note that $l_N(\boldsymbol{\lambda}) - l_M(\boldsymbol{\lambda}) = V_N(\boldsymbol{\lambda}) - V_M(\boldsymbol{\lambda})$ for any fixed $\boldsymbol{\lambda}$. In addition, note that the set of rounded coefficients $\mathcal{L}(\boldsymbol{\rho})$ contains at most $|\mathcal{L}(\boldsymbol{\rho})| \leq 2^d$ coefficients vectors. Therefore, in this setting, (19) implies that for any $\varepsilon > 0$,

$$\Pr\left(V_N(\boldsymbol{\lambda}) - V_M(\boldsymbol{\lambda}) \geq \varepsilon\right) \leq 2^d \exp\left(-\frac{2\varepsilon^2}{(\frac{1}{M})(1 - \frac{M}{N})(1 + \frac{M}{N})\Delta(\mathcal{L}(\boldsymbol{\rho}), \mathcal{D}_N)^2}\right). \quad (20)$$

By setting $\varepsilon = \varepsilon_\delta$ and simplifying the terms on the right hand side in (20), we can see that

$$\Pr\left(V_N(\boldsymbol{\lambda}) - V_M(\boldsymbol{\lambda}) \geq \varepsilon_\delta\right) \leq \delta.$$

Thus, the prescribed value of ε_δ ensures that $V_N(\boldsymbol{\lambda}) - V_M(\boldsymbol{\lambda}) \leq \varepsilon_\delta$ w.p. at least $1 - \delta$.

Since we have set ε_δ so that $V_N(\boldsymbol{\lambda}) - V_M(\boldsymbol{\lambda}) \leq \varepsilon_\delta$ w.p. at least $1 - \delta$, we now only need to show any $\boldsymbol{\lambda}$ that satisfies $V_M(\boldsymbol{\lambda}) < V^{\max} - \varepsilon_\delta$ will also satisfy $V_N(\boldsymbol{\lambda}) \leq V^{\max}$ to complete the proof. To see this, observe that:

$$\begin{aligned} V_N(\boldsymbol{\lambda}) - V_M(\boldsymbol{\lambda}) &\leq \varepsilon_\delta, \\ V_N(\boldsymbol{\lambda}) &\leq V_M(\boldsymbol{\lambda}) + \varepsilon_\delta, \\ V_N(\boldsymbol{\lambda}) &< V^{\max}. \end{aligned} \quad (21)$$

Here, (21) follows from the fact that $V_M(\boldsymbol{\lambda}) < V^{\max} - \varepsilon_\delta \implies V_M(\boldsymbol{\lambda}) + \varepsilon_\delta < V^{\max}$ ■

Appendix B. IP and LP Formulations

Basic Formulation for RiskSlimMIP and RiskSlimLP

$$
\begin{array}{lrcll}
\min\limits_{\theta,\boldsymbol{\lambda},\alpha} & \theta & + & C_0 \sum\limits_{j=1}^{d} \alpha_j & & \\
\text{s.t.} & \theta & \geq & l(\boldsymbol{\lambda}^t) + \langle \nabla l(\boldsymbol{\lambda}^t), \boldsymbol{\lambda} - \boldsymbol{\lambda}^t \rangle & t = 1,...,k & \textit{loss cuts} \quad (22a) \\
& \lambda_j & \leq & \Lambda_j^{\max} \alpha_j & j = 1,...,d & \textit{set } \ell_0 \textit{ indicator for +ve coefs} \quad (22b) \\
& \lambda_j & \geq & -\Lambda_j^{\min} \alpha_j & j = 1,...,d & \textit{set } \ell_0 \textit{ indicator for +ve coefs} \quad (22c) \\
& \theta & \geq & 0 & & \textit{approximate loss value} \quad (22d) \\
& \lambda_j & \in & \{\Lambda_j^{\min}, \ldots, \Lambda_j^{\max}\} & j = 1,...,d & \textit{coef. bounds} \quad (22e) \\
& \alpha_j & \in & \{0, 1\} & j = 1,...,d & \ell_0 \textit{ indicators} \quad (22f)
\end{array}
$$

We present an IP formulation for RiskSlimMIP in (22). The LP formulation for RiskSlimLP can be obtained by relaxing the integrality constraints in (22e) and (22f). This formulation contains $2d + 2$ constraints and $k + 2d$ variables. The approximate loss function is built through cuts constraints in (22a) as described in Section 3.1. Here, $\theta \in \mathbb{R}_+$ is an auxiliary variable that represents the value of the approximate loss function, and λ_j are coefficients that are bound to integer values in (22e). The ℓ_0-penalty is computed through binary indicator variables $\alpha_j = 1[\lambda_j \neq 0]$ in constraints (22b) and (22c).

Augmented Formulation for RiskSlimMIP and RiskSlimLP

$$
\begin{array}{lrcll}
\min\limits_{\theta,\boldsymbol{\lambda},\alpha} & V & & & & \\
\text{s.t.} & V & = & \theta + C_0 R & & \textit{objective value} \quad (23a) \\
& R & = & \sum\limits_{j=1}^{d} \alpha_j & & \ell_0 \textit{ norm} \quad (23b) \\
& \theta & \geq & l(\boldsymbol{\lambda}^t) + \langle \nabla l(\boldsymbol{\lambda}^t), \boldsymbol{\lambda} - \boldsymbol{\lambda}^t \rangle & t = 1,...,k & \textit{loss cuts} \quad (23c) \\
& \lambda_j & \leq & \Lambda_j^{\max} \alpha_j & j = 1,...,d & \textit{set } \ell_0 \textit{ indicator for +ve coefs} \quad (23d) \\
& \lambda_j & \geq & -\Lambda_j^{\min} \alpha_j & j = 1,...,d & \textit{set } \ell_0 \textit{ indicator for +ve coefs} \quad (23e) \\
& \lambda_j & \in & \{\Lambda_j^{\min}, \ldots, \Lambda_j^{\max}\} & j = 1,...,d & \textit{coefficient bounds} \\
& \alpha_j & \in & \{0, 1\} & j = 1,...,d & \ell_0 \textit{ indicators} \\
& V & \in & [V^{\min}, V^{\max}] & & \textit{objective bounds} \quad (23f) \\
& \theta & \in & [L^{\min}, L^{\max}] & & \textit{loss bounds} \quad (23g) \\
& R & \in & \{R^{\min}, \ldots, R^{\max}\} & & \ell_0 \textit{ bounds} \quad (23h)
\end{array}
$$

We present an IP formulation for the augmented version of RiskSlimMIP in (23). The LP formulation for the augmented version of RiskSlimLP can be obtained by relaxing the integrality constraints in (23f) and (23f). The augmented formulation in (23) includes 2 auxiliary variables: V which represents the objective value as per (23a); and R, which represents the ℓ_0-norm as per (23b). All other variables and constraints are identical to those in the formulation shown in (22). We use the auxiliary variables V, θ and R to bounds on the objective value, loss, and ℓ_0-norm in constraints (23f), (23g) and (23h), respectively. Note that we have purposely used auxiliary variables to bound the objective

value and ℓ_0 norm (as opposed to formulating a constraint using the variables) so that we can efficiently call the Chained Updates (Algorithm 5) in LCPA using CPLEX 12.6. This is because the *HeuristicCallback* in CPLEX can only change upper and lower bounds on individual variables in the MIP, but cannot change the LHS / RHS value of a constraint.

Appendix C. Details on Experimental Comparison with Simulated Data

C.1 Data Simulation Procedure

We simulated data from the `breastcancer` dataset (Mangasarian et al., 1995). The original dataset can be obtained from the UCI ML repository (Lichman, 2013), and has a total of $N = 683$ samples and $d = 9$ features $x_{ij} \in \{0, \ldots, 10\}$. Using the original dataset, we generated a collection of simulated datasets using the procedure outlined in Algorithm 7. Specifically, we first simulated the largest dataset we needed (with $N^{\max} = 10^6$ samples and $d^{\max} = 30$ features) by replicating features and samples from the original dataset and adding a small amount of normally distributed noise. Next, we created smaller datasets by taking *nested* subsets of the samples and the features. This ensured that any simulated dataset with d features and N samples contains all of the features and examples for a simulated dataset with $d' < d$ features and $N' < N$ samples. We designed this procedure to have the following special properties:

- It would produce difficult instances of the risk score problem. Here, RiskSlimMINLP instances for simulated datasets with $d > 9$ are challenging in terms of feature selection because they contain replicates of the original 9 features, which are strongly correlated with each another. Feature selection becomes exponentially harder when collections of highly correlated features are used, since this means that there are an exponentially larger number of slightly suboptimal solutions.

- We could make inferences about the optimal objective value of RiskSlimMINLP instances we may not have been able to solve. Say, for example, that we could not solve an instance of the risk score problem for the simulated dataset with $(d, N) = (20, 10^6)$, but could solve an instance for the simulated dataset with $(d, N) = (10, 10^6)$. In this case, we knew that the optimal objective value of the $(d, N) = (20, 10^6)$ instance had to be less than or equal to the optimal objective value of the $(d, N) = (10, 10^6)$ instance because the $(d, N) = (20, 10^6)$ dataset contained all of the features as the $(d, N) = (10, 10^6)$ dataset.

C.2 Implementation Details

We fit risk scores for all datasets by formulating an RiskSlimMINLP instance where $C_0 = 10^{-5}$, $\lambda_0 \in \{-100, 100\}$, and $\lambda_j = -10, \ldots, 10$ for $j = 1, \ldots, d$. We solved this instance using the following techniques: (i) CPA (Algorithm 1); (ii) LCPA (Algorithm 2); (iii) an active set MINLP algorithm; (iv) an interior direct MINLP algorithm; (v) an interior CG MINLP algorithm. We solved all instances on a 3.33 GHz Intel Xeon CPU with 16GB of RAM and capped total runtime to 6 hours. If an algorithm could not solve the problem to optimality within the 6 hour time limit, we reported results based on the best feasible solution it found. We implemented both CPA and LCPA using the CPLEX 12.6.3 API, which we accessed using the Python API. We solved instances using MINLP algorithms using the Artelsys Knitro 9.0 MINLP solver (Byrd et al., 2006), which we accessed through MATLAB 2015b.

Algorithm 7 Simulation Procedure

Input

$X^{\text{original}} = [x_{ij}]_{i=1\ldots N^{\text{original}}, j=1\ldots d^{\text{original}}}$ — feature matrix of original dataset

$Y^{\text{original}} = [y_i]_{i=1\ldots N^{\text{original}}}$ — label matrix of original dataset

$d^1 \ldots d^{\max}$ s.t. $0 < d^1 < \ldots < d^{\max}$ — desired dimensions for simulated datasets

$N^1 \ldots N^{\max}$ s.t. $0 < N^1 < \ldots < N^{\max}$ — desired sample sizes for simulated datasets

---

$\mathcal{J}^{\text{original}} = [1, \ldots, d^{\text{original}}]$ — index array for original features

$\mathcal{J}^{\max} \leftarrow []$ — index array of features for largest simulated dataset

$m^{\text{full}} \leftarrow \lfloor d^{\max} / d^{\text{original}} \rfloor$

$m^{\text{remainder}} \leftarrow d^{\max} - d^{\text{original}}$

Step I: Generate Largest Dataset

for $m = 1, \ldots, m^{\text{full}}$ **do**
  $\mathcal{J}^{\max} \leftarrow [\mathcal{J}^{max}, \mathsf{RandomPermute}(\mathcal{J}^{\text{original}})]$
end for
$\mathcal{J}^{\max} \leftarrow [\mathcal{J}^{max}, \mathsf{RandomSampleWithoutReplacement}(\mathcal{J}^{\text{original}}, m^{\text{remainder}})]$

for $i = 1, \ldots, N^{\max}$ **do**
  sample l with replacement from $1, \ldots N^{\text{original}}$
  $y_i^{\max} \leftarrow y_i$
  for $j = 1, \ldots, d^{\max}$ **do**
    $k \leftarrow \mathcal{J}^{\max}[j]$
    sample ε from Normal$(0, 0.5)$
    $x_{ij}^{\max} \leftarrow \lceil x_{l,k} + \varepsilon \rfloor$ ▷ new features are noisy versions of original features
    $x_{ij}^{\max} \leftarrow \min(10, \max(0, x_{ij}^{\max}))$ ▷ new features have same bounds as old features
  end for
end for
$X^{\max} \leftarrow [x_{ij}]_{i=1\ldots N^{\max}, j=1\ldots d^{\max}}$
$Y^{\max} \leftarrow [y_i^{max}]_{i=1\ldots N^{\max}}$

Step II: Generate Smaller Datasets

for $d = [d^1, \ldots, d^{\max}]$ **do**
  for $N = [N^1, \ldots, N^{\max}]$ **do**
    $X^{(N,d)} = X^{\max}[1:N, 1:d]$
    $Y^N = Y^{\max}[1:N]$
  end for
end for

Output: simulated datasets $(X^{(N,d)}, Y^N)$ for all $N^1 \ldots N^{\max}$ and $d^1 \ldots d^{\max}$.

C.3 Results for All MINLP Algorithms

We examined the performance of 3 MINLP algorithms in Artelsys Knitro 9.0, namely: an active set algorithm (MINLP Active Set); an interior-point algorithm (MINLP Interior); an interior-point algorithm where the primal-dual KKT system is solved with a conjugate gradient method (MINLP Interior CG). We only show results from MINLP Active Set in Figure 6 because all three algorithms behave similarly. For completeness, we include the same plots for the remaining MINLP algorithms in Figure 19.

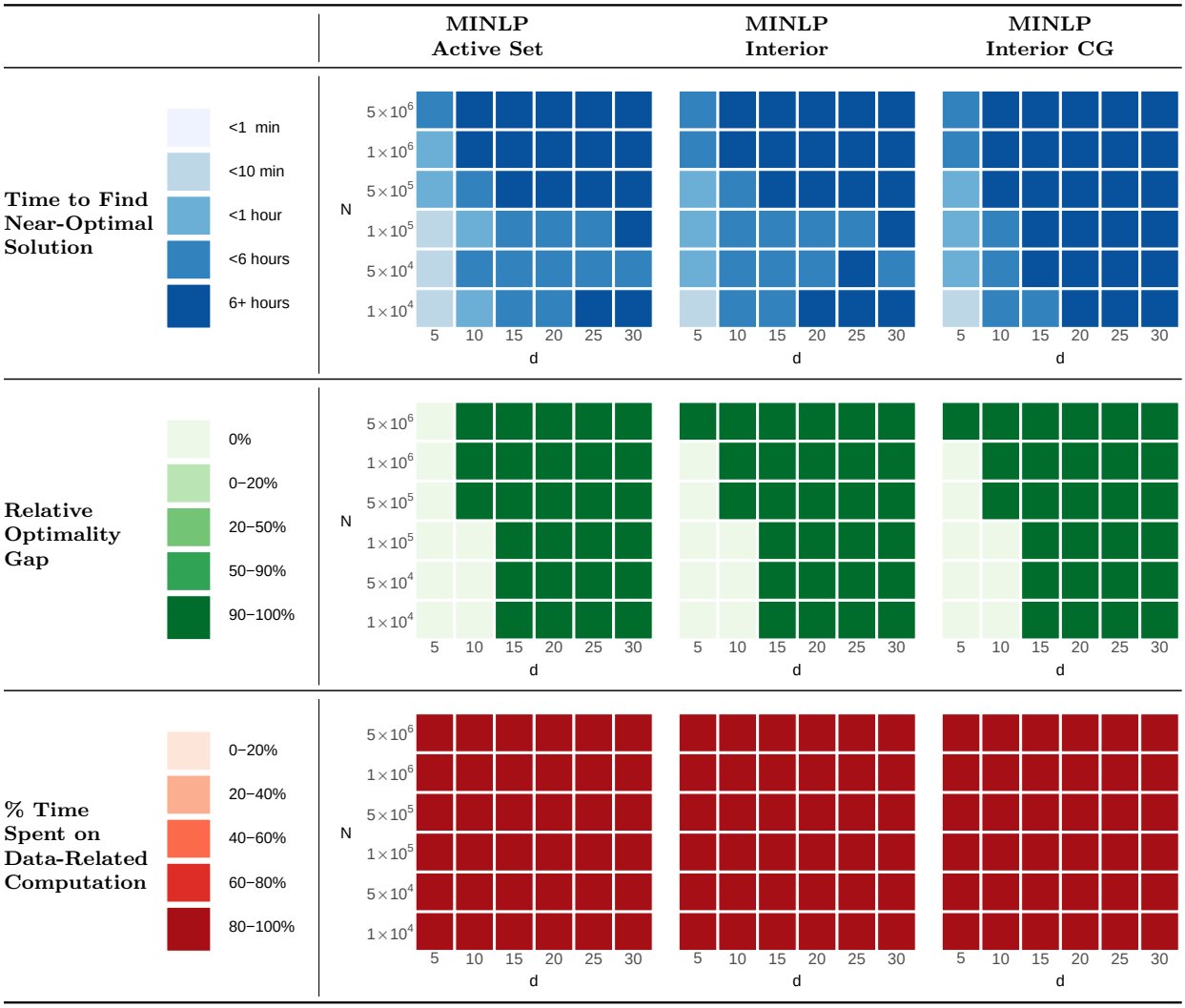

Figure 19: Performance of MINLP algorithms to solve RiskSlimMINLP on simulated datasets with varying dimensions d and sample sizes N. All algorithms perform similarly. We report results from MINLP Active Set in Figure 6 because it solves the most instances to optimality.